Combined Analysis

Applied to thin layer architectures

Daniel Chateigner

IUT-Univ. Caen Basse-Normandie

CRISMAT-ENSICAEN (Caen-France)

UTT, 19th June 2012

Structure determination on real (textured) samples
Dilemma 1

Structure and QTA: correlations ?

f(g) and $|F_h|^2$ are different !

f(g):

-Angularly constrained: $[h_1k_1l_1]^*$ and $[h_2k_2l_2]^*$ make a given angle: more determined if F^2 high

- lot of data (spectra) needed

$|F_h|^2$:

-Position, f_i, and Debye-Waller constrained

- work on the sum of all diagrams on average

Texture from Spectra

Orientation Distribution Function (ODF)

From pole figures

From spectra

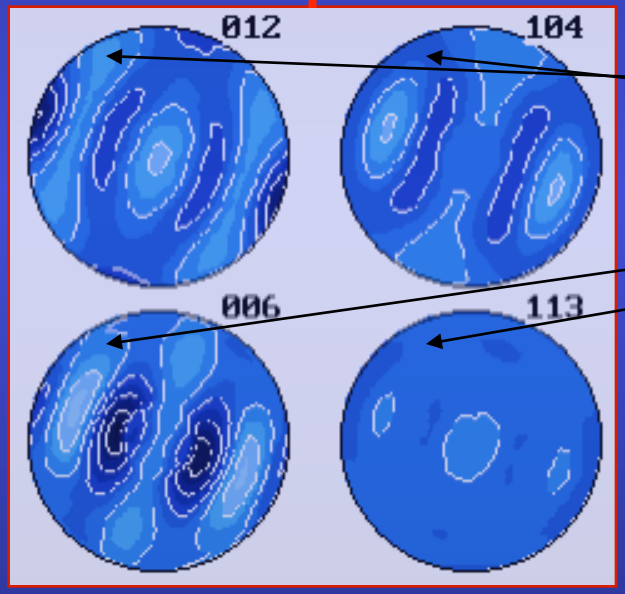

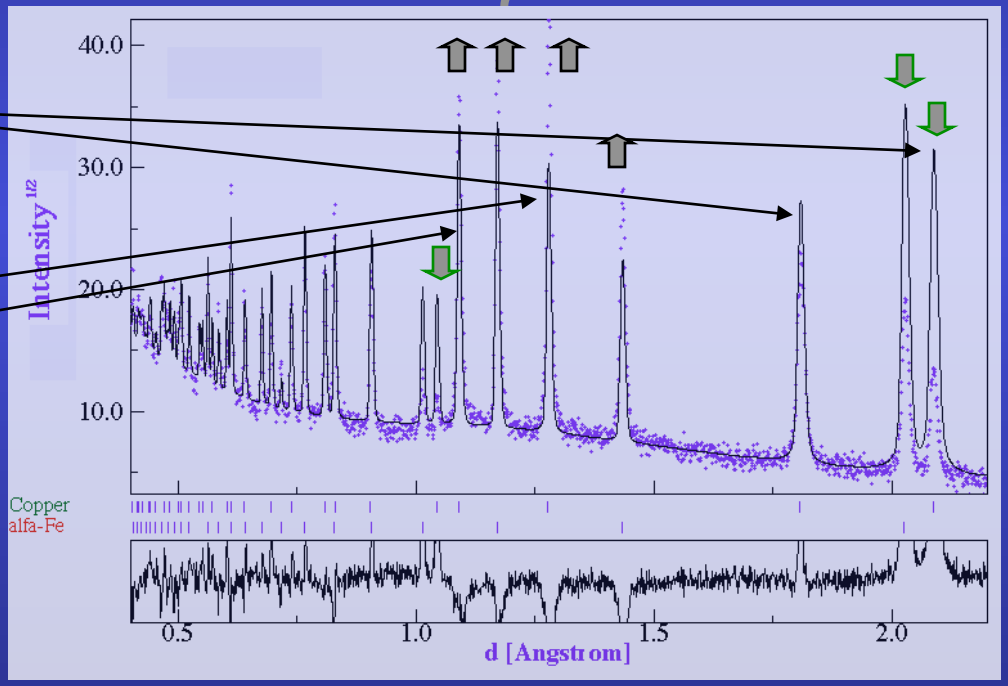

Le Bail extraction + ODF: WMV, E-WIMV, Generalized spherical harmonics, components, ADC, entropy maximisation …

Why not benefit of texture in Structure determination ?

Perfect powders:

- overlaps (intra- and inter-p
- no angular constrain
- anisotropy difficult to resc

Single crystals:

- reduced overlaps
- max angular constrains
- Perfect texture: max anisotropy

Single pattern

Many individual diffracted peaks

Textured powders:

- reduced overlaps
- angular constrain = f(texture strength)
- Intermediate anisotropy

Many patterns to measure and analyse

Rietveld-Structure

$$I_i^{calc}(\chi,\phi) = \sum_{n=1}^{Nphases} S_n \sum_k L_k \left|F_{k;n}\right|^2 S(2\theta_i - 2\theta_{k;n}) P_{k;n}(\chi,\phi) A + bkg_i$$

Texture

$$P_k(\chi,\phi) = \int_{\varphi} f(g,\varphi) d\varphi$$

- Generalized Spherical Harmonics (Bunge):

$$P_k(\chi,\phi) = \sum_{l=0}^{\infty} \frac{1}{2l+1} \sum_{n=-l}^{l} k_l^n(\chi,\phi) \sum_{m=-l}^{l} C_l^{mn} k_n^{*m}(\Theta_k \phi_k)$$

$$f(g) = \sum_{l=0}^{\infty} \sum_{m,n=-l}^{l} C_l^{mn} T_l^{mn}(g)$$

- Components (Helming):

$$f(g) = F + \sum_c I^c f^c(g)$$

- WIMV (William, Imhof, Matthies, Vinel) iterative process:

$$f^{n+1}(g) = N_n \frac{f^n(g) f^0(g)}{\left(\prod_{h=1}^{I} \prod_{m=1}^{M_h} P_h^n(y) \right)^{\frac{1}{IM_h}}}$$

$$f^0(g) = N_0 \left(\prod_{h=1}^{I} \prod_{m=1}^{M_h} P_h^{exp}(y) \right)^{\frac{1}{IM_h}}$$

E-WIMV (Rietveld only):

with $0 < r_n < 1$, relaxation parameter,
M_h number of division points of the integral around k,
w_h reflection weight

$$f^{n+1}(g) = f^n(g) \prod_{m=1}^{M_h} \left(\frac{P_h(y)}{P_h^n(y)} \right)^{r_n \frac{w_h}{M_h}}$$

- Entropy maximisation (Schaeben):

$$f^{n+1}(g) = f^n(g) \prod_{m=1}^{M_h} \left(\frac{P_h(y)}{P_h^n(y)} \right)^{\frac{r_n}{M_h}}$$

- arbitrarily defined cells (ADC, Pawlik): Very similar to E-WIMV, with integrals along path tubes

Residual Stresses shift peaks with **y**

Dilemma 2

Stress and QTA: correlations ? f(g) and $\langle C_{ijkl} \rangle$

f(g):

- Moves the $\sin^2\Psi$ law away from linear relationship
- Needs the integrated peak (full spectra)

strains:

- Measured with pole figures
- needs the mean peak position

Isotropic samples: triaxial, biaxial, uniaxial stress states

Textured samples: Reuss, Voigt, Hill, Bulk geometric mean approaches

Residual Stresses and Rietveld

- Macro elastic strain tensor (I kind)
- Crystal anisotropic strains (II kind)

C

Macro and micro stresses

Applied macro stresses

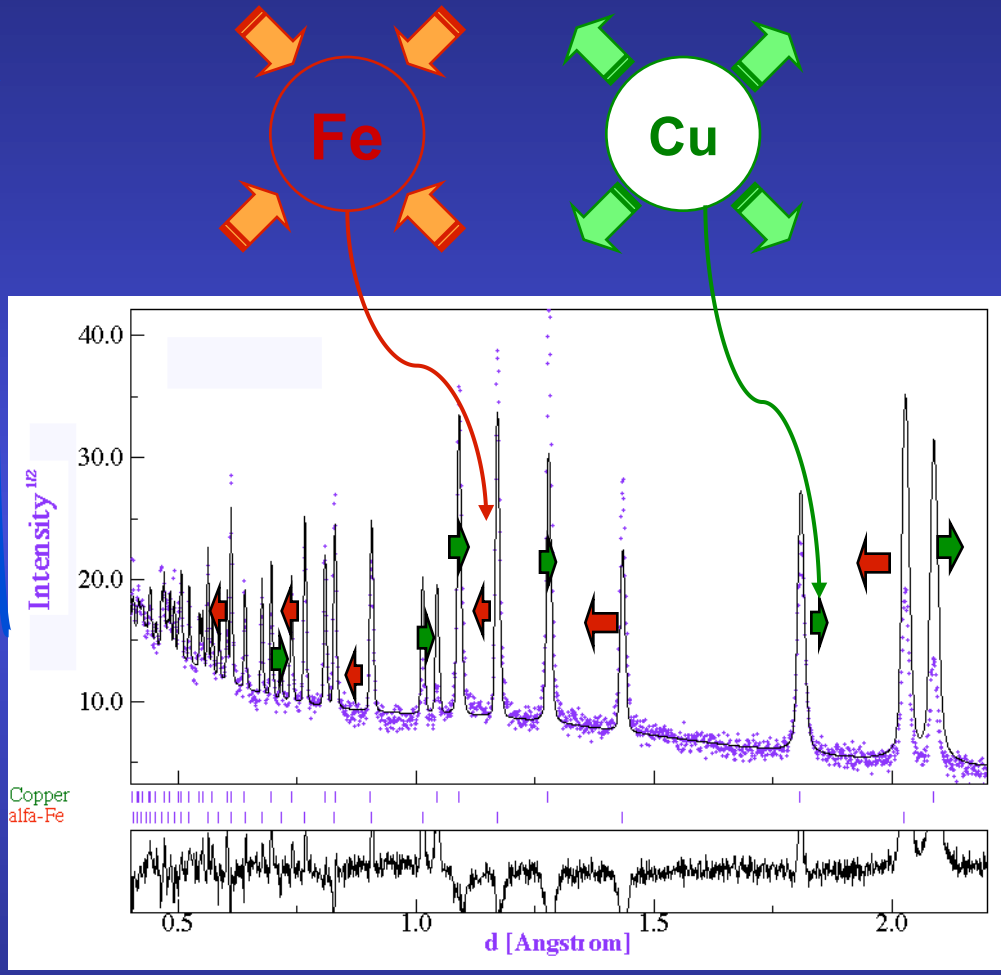

Isotropic samples: triaxial, biaxial, uniaxial stress states

Textured samples: Reuss, Voigt, Hill, Bulk geometric mean approaches

Strain-Stress

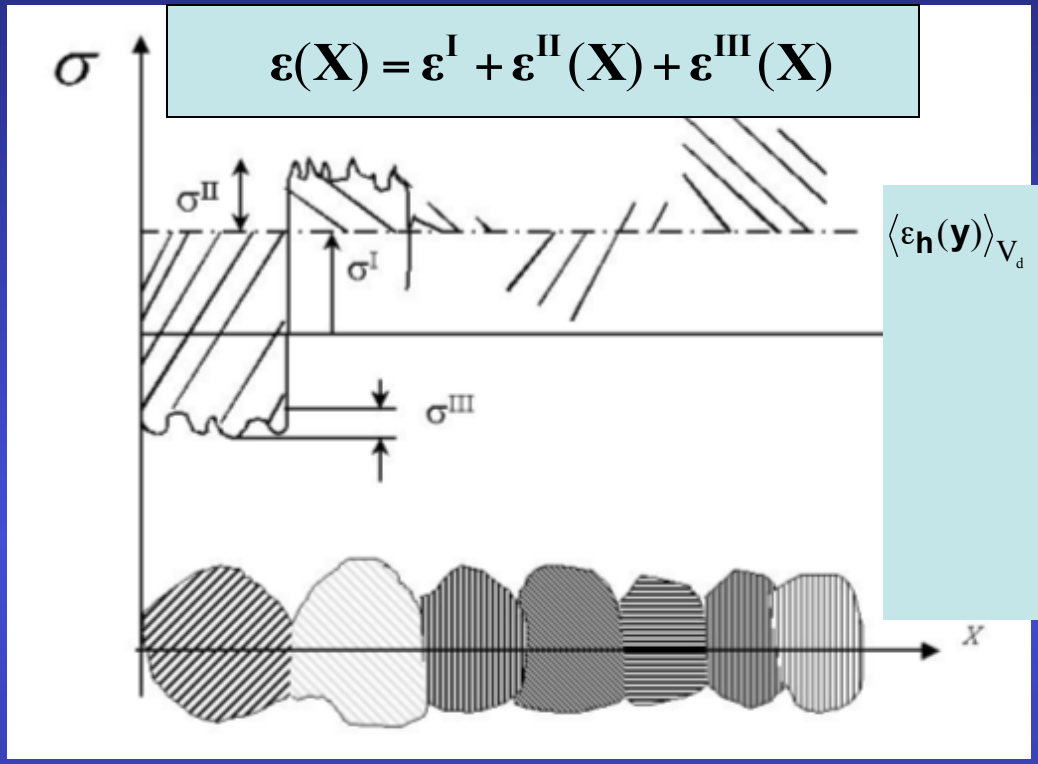

$$\boldsymbol{\varepsilon}(\mathbf{X}) = \boldsymbol{\varepsilon}^{\mathbf{I}} + \boldsymbol{\varepsilon}^{\mathbf{II}}(\mathbf{X}) + \boldsymbol{\varepsilon}^{\mathbf{III}}(\mathbf{X})$$

Isotropic samples:
triaxial, biaxial uniaxial stress state

$$\langle \varepsilon_{\mathbf{h}}(\mathbf{y}) \rangle_{V_d} = \frac{1}{V_d} \int_{V_d} (\varepsilon_{33}^{I} + \varepsilon_{33}^{II} + \varepsilon_{33}^{III}) dV$$

$$= (\varepsilon_{11}^{I} \cos^2\phi + \varepsilon_{12}^{I} \sin 2\phi + \varepsilon_{22}^{I} \sin^2\phi - \varepsilon_{33}^{I}) \sin^2\psi + \varepsilon_{33}^{I} +$$

$$(\varepsilon_{13}^{I} \cos\phi + \varepsilon_{23}^{I} \sin\phi) \sin 2\psi + \frac{1}{V_d} \int_{V_d} (\varepsilon_{33}^{IIe} + \varepsilon_{33}^{IIti} + \varepsilon_{33}^{IIpi}) dV$$

$$= \frac{\langle d(hkl,\phi,\psi) \rangle_{V_d} - d_0(hkl)}{d_0(hkl)}$$

Textured samples:
triaxial, biaxial uniaxial stress state
+ ODF + SDF + model

$$\langle E(\mathbf{g}) \rangle_{V_d} = \frac{1}{V_d} \int_{V_d} E^{SC}(g) f(g) dg$$

$$= \left(\prod_{V_d} E^{SC}(g) f(g) dg \right)^{\frac{1}{V_d}}$$

$$\chi^2 = \sum_i w_i^2 \left[\varepsilon_i^{calc}(S_{ijk\ell}^M, \mathbf{h}, \mathbf{y}) - \varepsilon_i^{meas}(S_{ijk\ell}^M, \mathbf{h}, \mathbf{y}) \right]^2$$

Non-linear least-square fit

Layered systems
Dilemma 3

Layer, Rietveld and QTA: correlations: f(g), thicknesses and structure

f(g):
- Pole figures need corrections for abs-vol
- Rietveld also to correct intensities

layers:
- unknown sample true absorption coefficient μ
- unknown effective thickness (porosity)

Layering

Asymmetric Bragg-Brentano

$$C_{\chi}^{\text{top film}} = g_1\left(1-\exp\left(-\mu T g_2/\cos\chi\right)\right)/\left(1-\exp\left(-2\mu T/\sin\omega\cos\chi\right)\right)$$

$$C_{\chi}^{\text{cov. layer}} = C_{\chi}^{\text{top film}}\left(\exp\left(-g_2\sum\mu_i' T_i'/\cos\chi\right)\right)/\left(\exp\left(-2\sum\mu_i' T_i'/\sin\omega\cos\chi\right)\right)$$

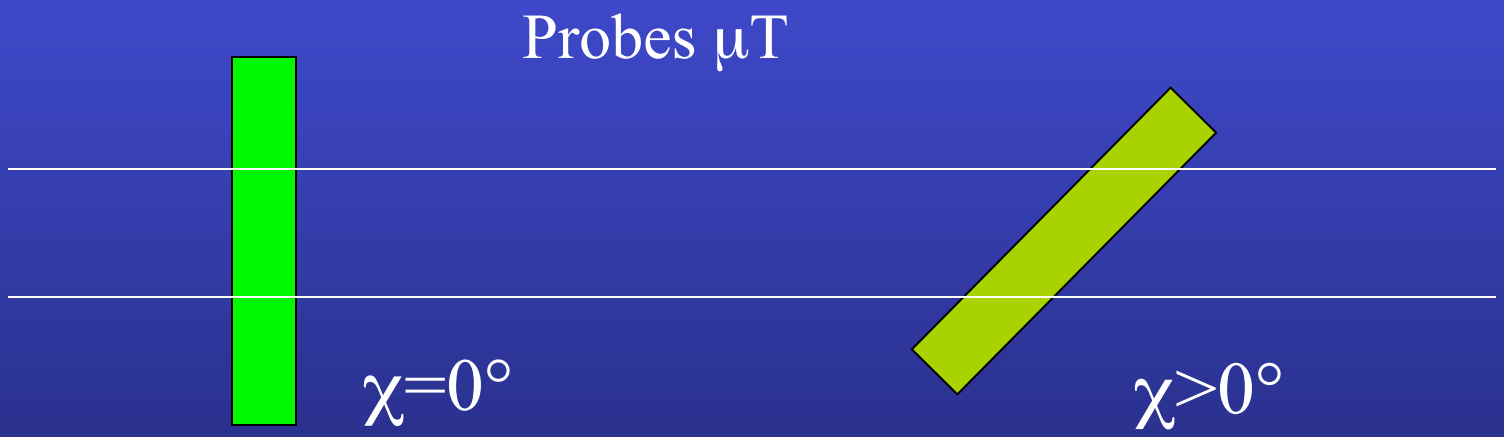

Phase and Texture
Dilemma 4

Phase and QTA: correlations: f(g), S_Φ

f(g):
- angular relationships
- plays on individual spectra
- essential to operate on textured sample

S_Φ:
- plays on overall scale factor (sum diagram)

Phase analysis

- Volume fraction

$$V_\Phi = \frac{S_\Phi V_{uc\Phi}^2}{\sum_\Phi \left(S_\Phi V_{uc\Phi}^2\right)_\Phi}$$

- Weight fraction

$$m_\Phi = \frac{S_\Phi Z_\Phi M_\Phi V_{uc\Phi}^2}{\sum_\Phi \left(S_\Phi Z_\Phi M_\Phi V_{uc\Phi}^2\right)_\Phi}$$

Z = number of formula units

M = mass of the formula unit

V = cell volume

How it works

Le Bail extraction

$$T_{hkl}^{k} = T_{hkl}^{k-1} \frac{\sum_i I_i^{exp} S_{hkl}^{i}}{\sum_i I_i^{calc} S_{hkl}^{i}}$$

- Starts with nominal intensities (T_{hkl})
- Computes the full pattern (I^{calc})
- Uses the formula to compute next T_{hkl}
- Cycle the last two steps until convergence

- In Maud, options:
  - Only few cycles for texture (3-5) necessary
  - The range for the weighting of the profile can be reduced
  - Background subtracted or not

Structure and Residual Stresses (shift peaks with **y**)
Dilemma 5

Stress and cell parameters: correlations: peak positions and C_{ijkl}

Cell parameters:
- Measured at high angles
- Bragg law evolution

strains:
- Measured precisely at high angles
- stiffness-based variation, also with Ψ

Shapes, microstrains, defaults, distributions
Dilemma 6

Shapes …. and stress-texture-structure: correlations ?

Shapes …:
- line broadening problem
- average positions modified
- if anisotropic: modification changes with **y**

Stress-texture-structure:
- need “true” peak positions and intensities
- need deconvoluted signals

Scherrer, Integral breadth, Williamson-Hall …

$$\langle D \rangle_v = \frac{K\lambda}{\beta_S(2\theta)\ \cos\theta}$$

More elegant, mandatory for whole-pattern: Stokes deconvolution
Bertaut-Warren-Averbach treatment, e.g. for a 00l peak:

$$A_n = A_n^S A_n^D = \frac{N_n}{N_3}\langle \cos 2\pi l Z_n \rangle$$

$$A_n^S = \frac{N_n}{N_3} = \frac{1}{N_3}\sum_{i=|n|}^{\inf}(i-|n|)p(i)$$

$$\left(\frac{dA_n^S}{dn}\right)_{n\to 0} = -\frac{1}{N_3}$$

Second derivative: distribution of column lengths

Anisotropic sizes and microstrains

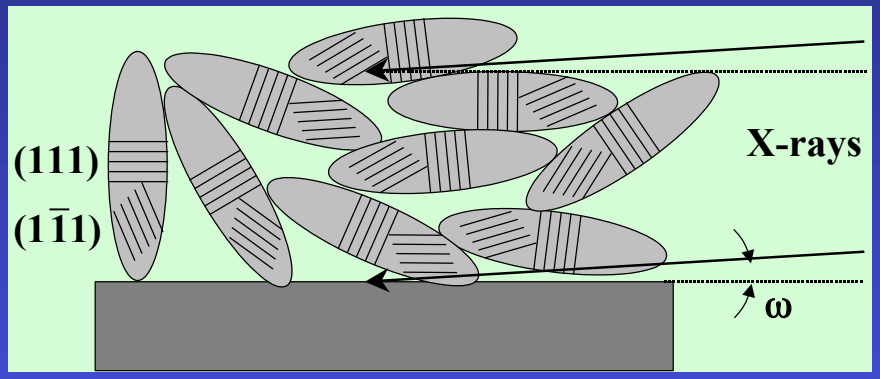

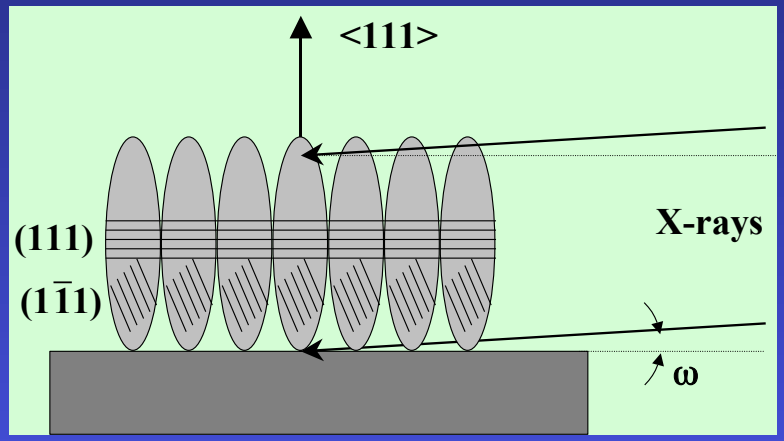

- Texture helps the "real" mean shape determination
- Determination by peak deconvolution + Popa formalism

$$\langle R_h \rangle = R_0 + R_1 P_2^0(x) + R_2 P_2^1(x)\cos\varphi + R_3 P_2^1(x)\sin\varphi + R_4 P_2^2(x)\cos 2\varphi + R_5 P_2^2(x)\sin 2\varphi +$$

$$\langle \varepsilon_h^2 \rangle E_h^4 = E_1 h^4 + E_2 k^4 + E_3 \ell^4 + 2E_4 h^2 k^2 + 2E_5 \ell^2 k^2 + 2E_6 h^2 \ell^2 + 4E_7 h^3 k + 4E_8 h^3 \ell + 4E_9 k^3 h + 4E_{10} k^3 \ell + 4E_{11} \ell^3 h + 4E_{12} \ell^3 k + 4E_{13} h^2 k \ell + 4E_{14} k^2 h \ell + 4E_{15} \ell^2 k h$$

$\bar{1}$

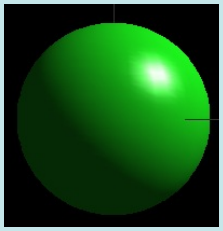

R_0

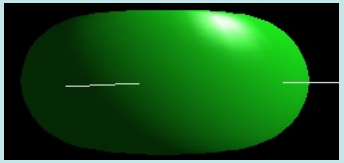

R_0, $R_1 < 0$

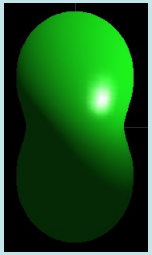

R_0, $R_1 > 0$

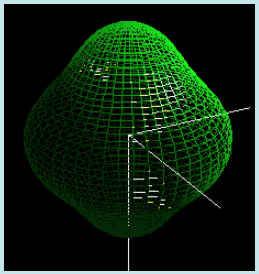

R_0, $R_6 > 0$

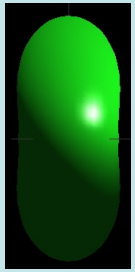

R_0,
R_2 and $R_6 > 0$

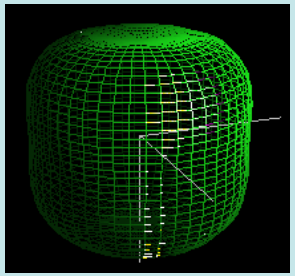

R_0, $R_6 < 0$

6/m

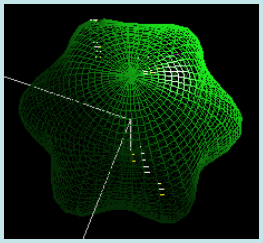

R_0, $R_4 > 0$

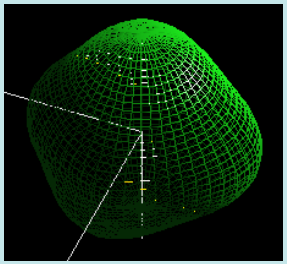

R_0, $R_1 > 0$

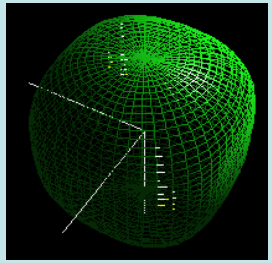

R_0, $R_1 < 0$

m3m

Gold thin films

Crystallite size (Å) along	Film thickness					
	10nm	15nm	20nm	25nm	35nm	40nm
[111]	176	153	725	254	343	379
[200]	64	103	457	173	321	386
[202]	148	140	658	234	337	381

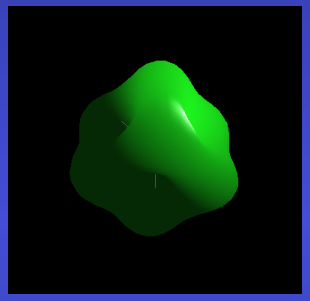

10 nm

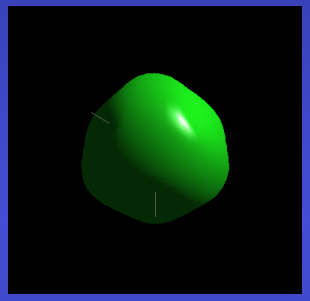

15 nm

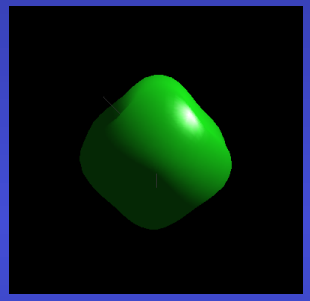

20 nm

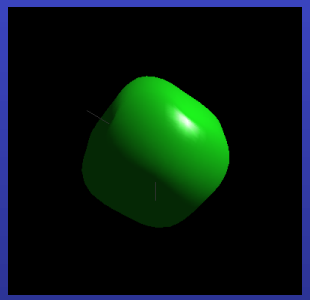

25 nm

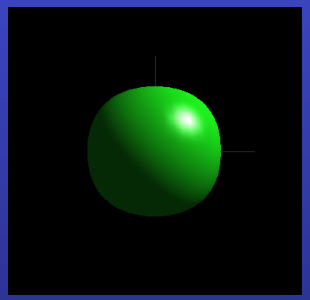

35 nm

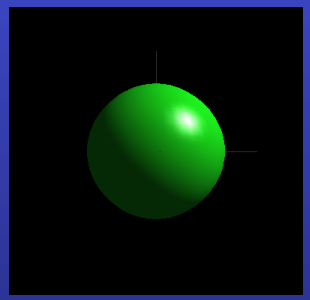

40 nm

EMT nanocrystalline zeolite

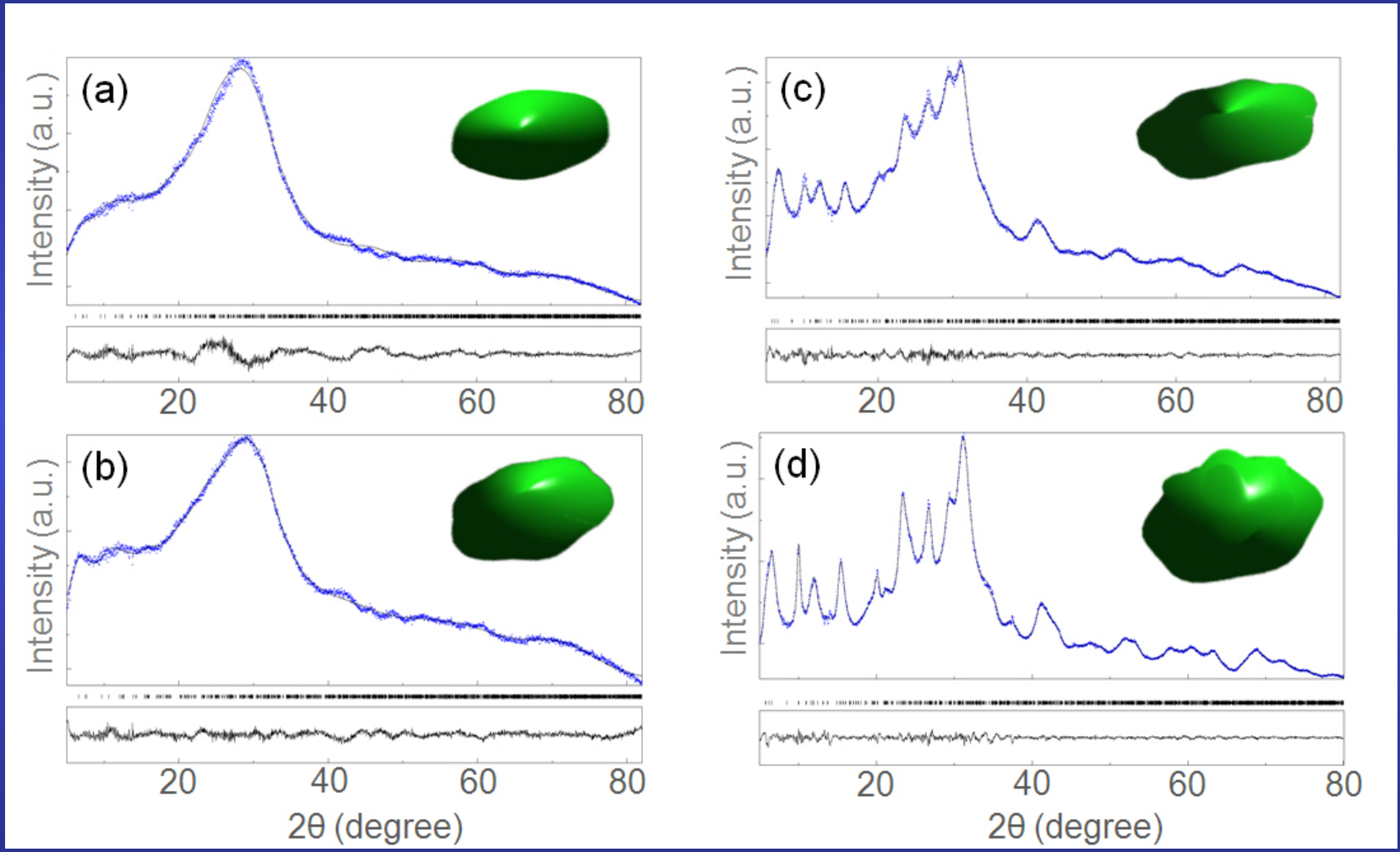

Combined Analysis approach

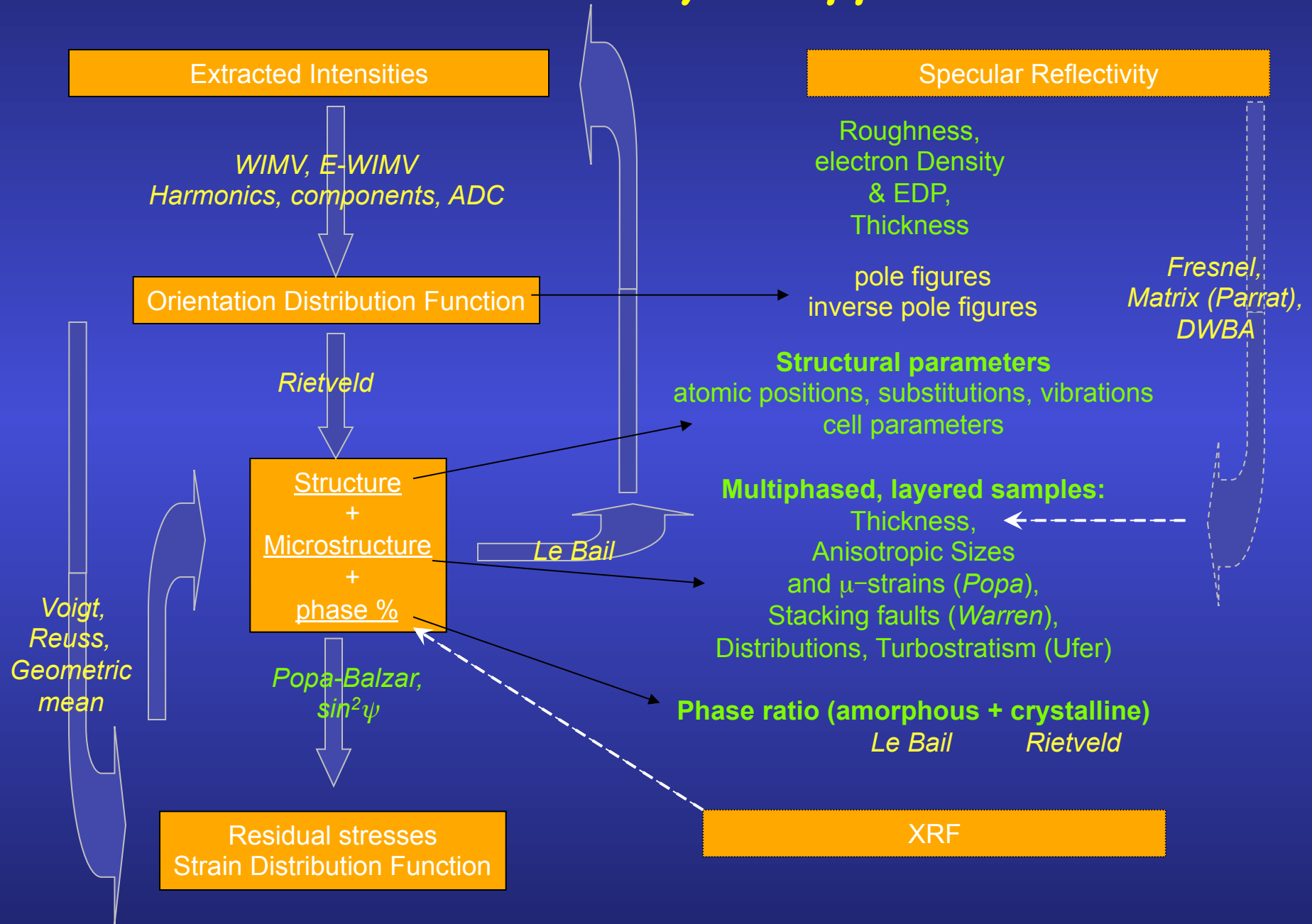

Grinding to powderise another dilemma !

Grinding: removes angular relationship, adds correlations

Texture:
- not measured
- removed ? hope to get a perfect powder

Strains, defaults, anisotropy … :
- some removed, some added

Same sample ?

Rare samples ?

Minimum experimental requirements

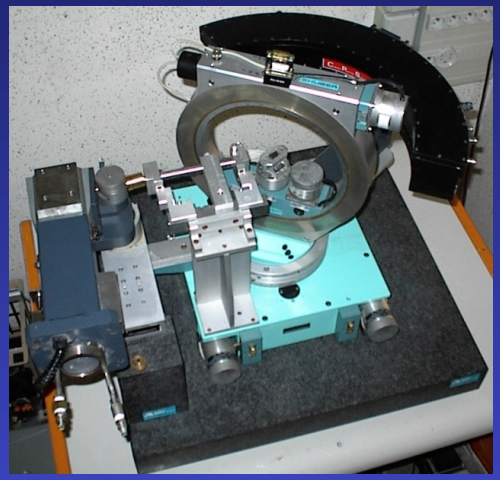

1D or 2D Detector + 4-circle diffractometer
(X-rays and neutrons)
CRISMAT, ILL

+

~1000 experiments (2θ diagrams)
in as many sample orientations

+

Instrument calibration
(peaks widths and shapes,
misalignments, defocusing …)

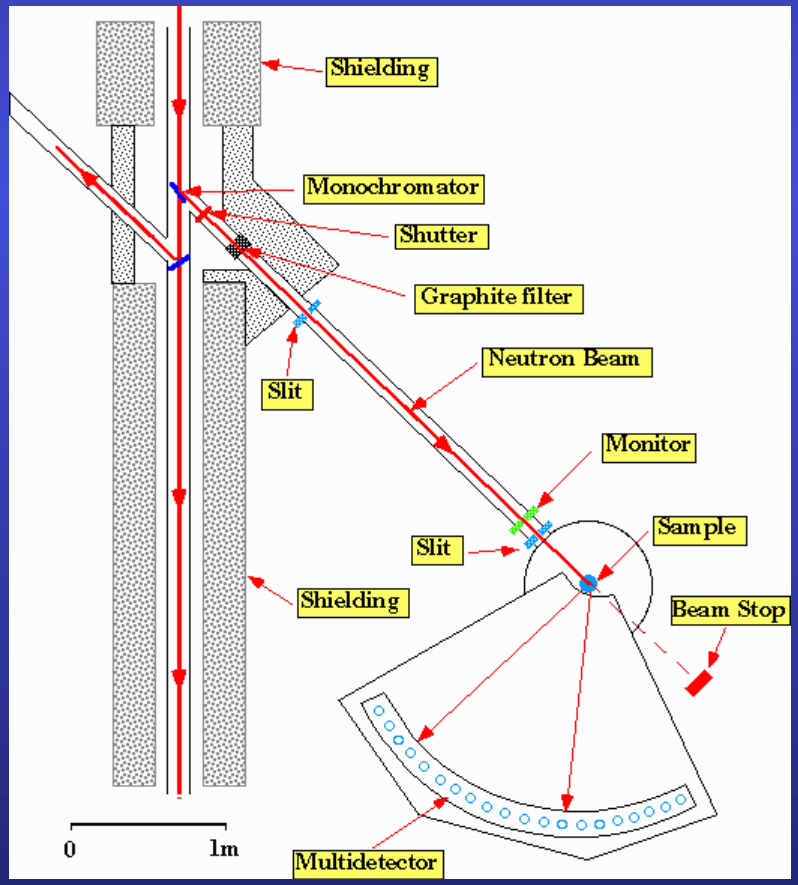

2D Curved Area Position Sensitive Detector

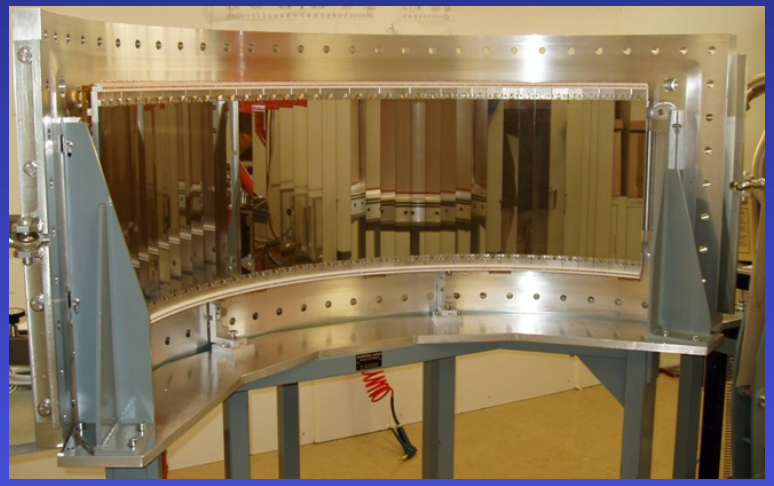

D19 - ILL

+

~100 experiments (2D Debye-Scherrer diagrams)

in as many sample orientations

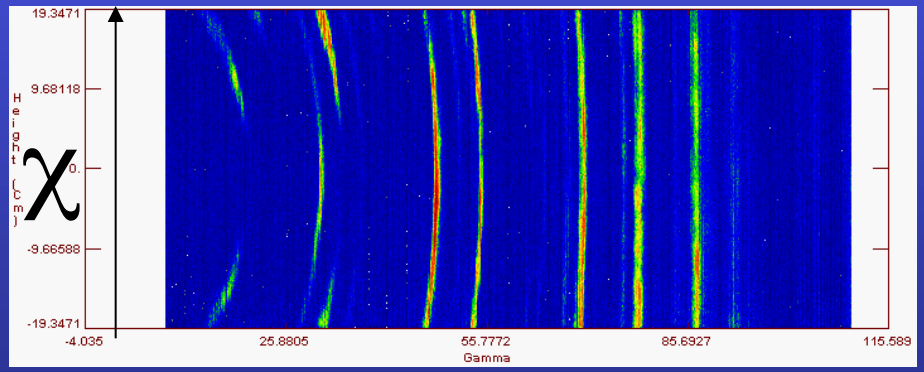

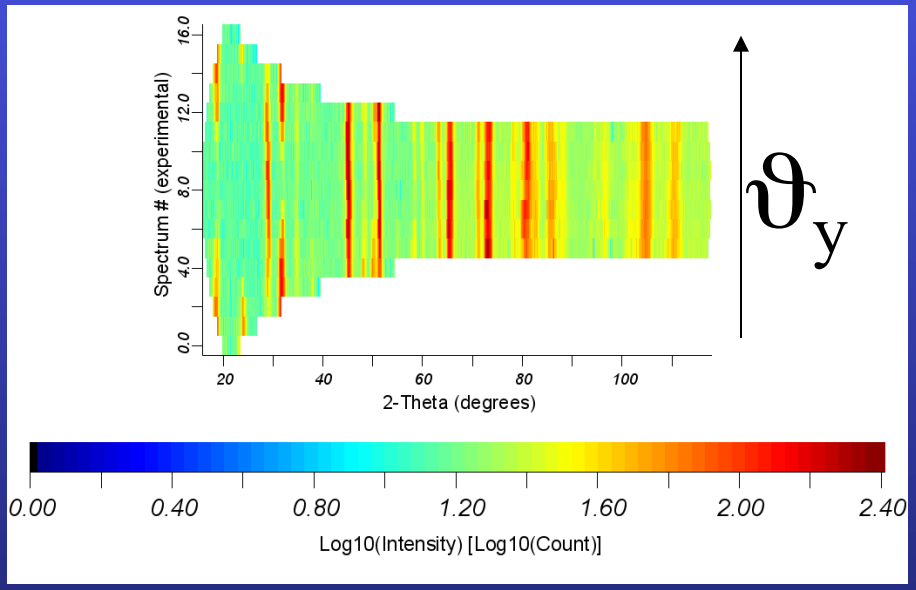

Calibration

ω = 20°

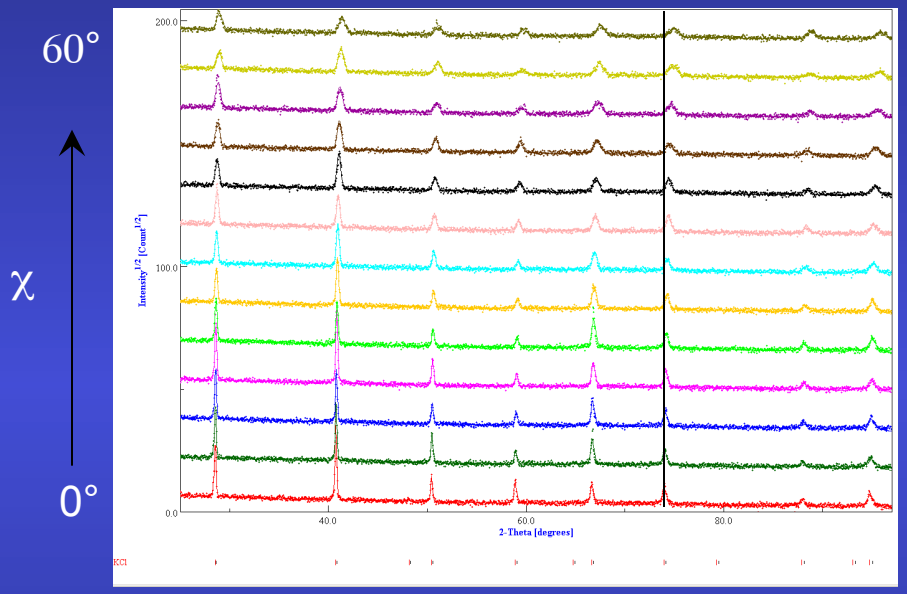

ω = 40°

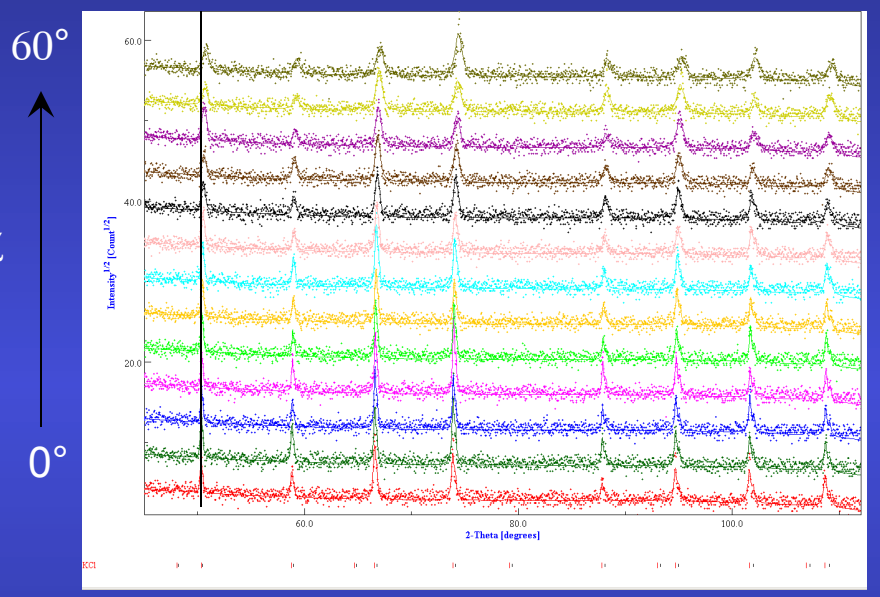

KCl, LaB_6 …

→

FWHM (ω, χ, 2θ …)
2θ shift
gaussianity
asymmetry
misalignments ...

Minimization algorithms

- Can be fully used in the method (everywhere)

- Marquardt Least Squares (based on steepest decrease and Gauss-Newton)
  - Efficient, best with few parameters, near the solution
- Evolutionary computation (or genetic algorithm)
  - Slow, not efficient, requires a lot of resources
  - Unlimited number of parameters
  - Can start far from the solution
- Simulated annealing (the solution proceed like a random walk, but the walking step decreases as temperature decreases)
  - In between the Marquardt and evolutionary algorithms
- Simplex (generates n+1 starting solutions as vertices of a polygon, n number of parameters, and contract/expand the polygon around the minima)
  - Slow on convergence
  - Remains close to the solution, but explore more minima with respect to the Marquardt

Ferroelectric PCT films

J. Ricote, Madrid

thin films:

$(Ca_{0.24}Pb_{0.76})TiO_3$ sol-gel synthesised solutions deposited by spin coating on a substrate of $Pt/TiO_2/Si$, with and without a treatment at 650ºC for 30 min.

All films are crystallised at 700ºC for 50 s by Rapid Thermal Processing (RTP; 30ºC/s). A series is also recrystallised at 650ºC for 1 to 3 h.

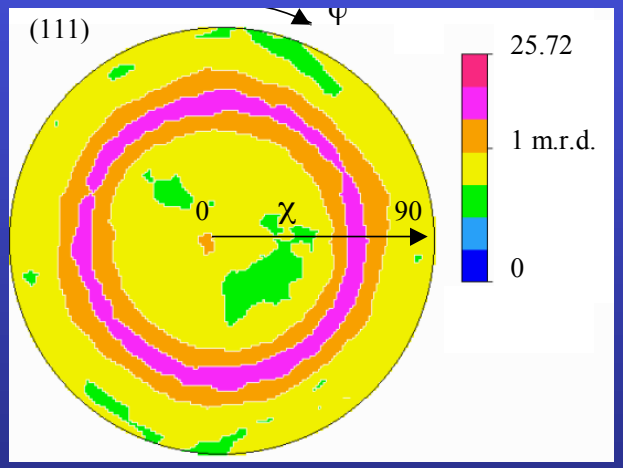

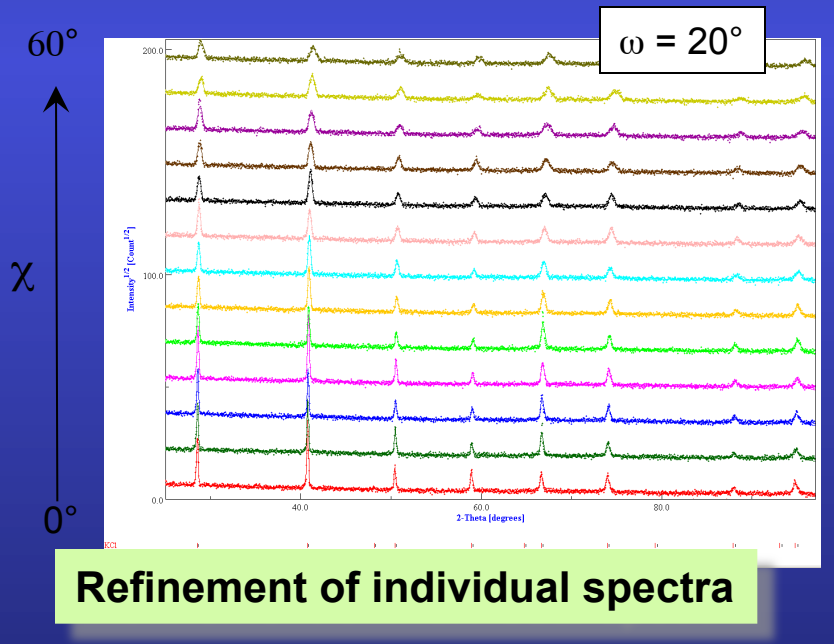

Refinement of individual spectra

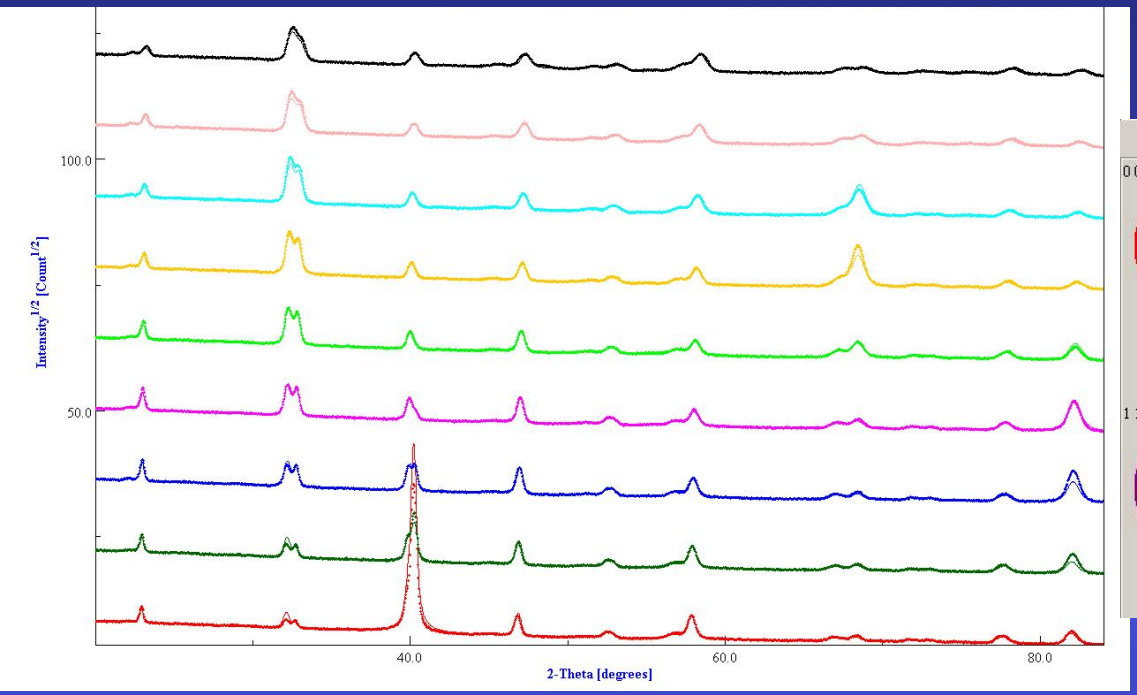

PCT

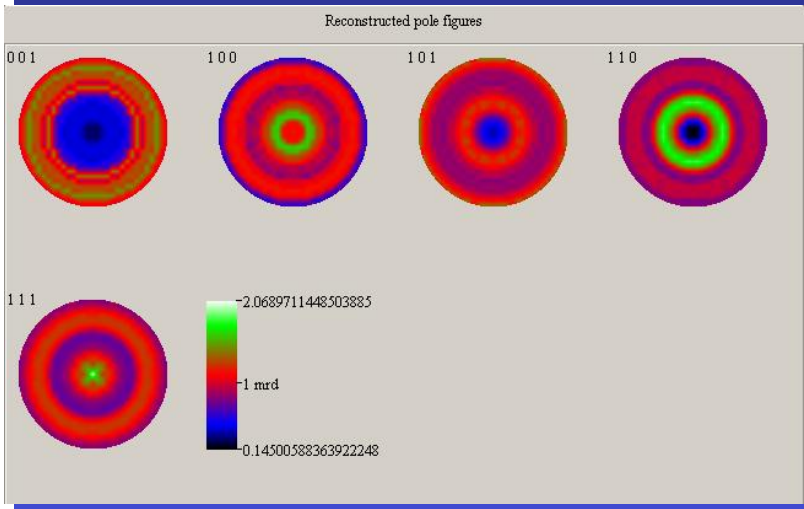

a = 3.9156(1) Å
c = 4.0497(3) Å
T = 2525(13) Å
t_{iso} = 390(7) Å
ε = 0.0067(1) rms

Pt

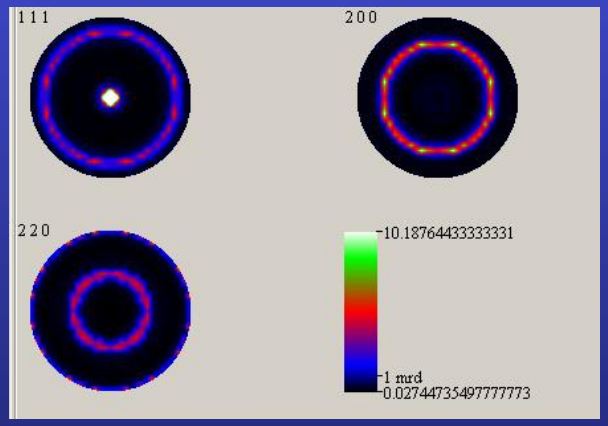

a = 3.9108(1) Å
T = 457(3) Å
t_{iso} = 458(3) Å
ε' = 0.0032(1) rms

R_W = 13%; R_B = 12%; R_{exp} = 22%.(Rietveld)
R_W = 5%; R_B = 6% (E-WIMV)

Atom	Occupancy	x	y	z
Pb	0.76	0.0	0.0	0.0
Ca	0.24	0.0	0.0	0.0
Ti	1.0	0.5	0.5	0.477(2)
O1	1.0	0.5	0.5	0.060(2)
O2	1.0	0.0	0.5	0.631(1)

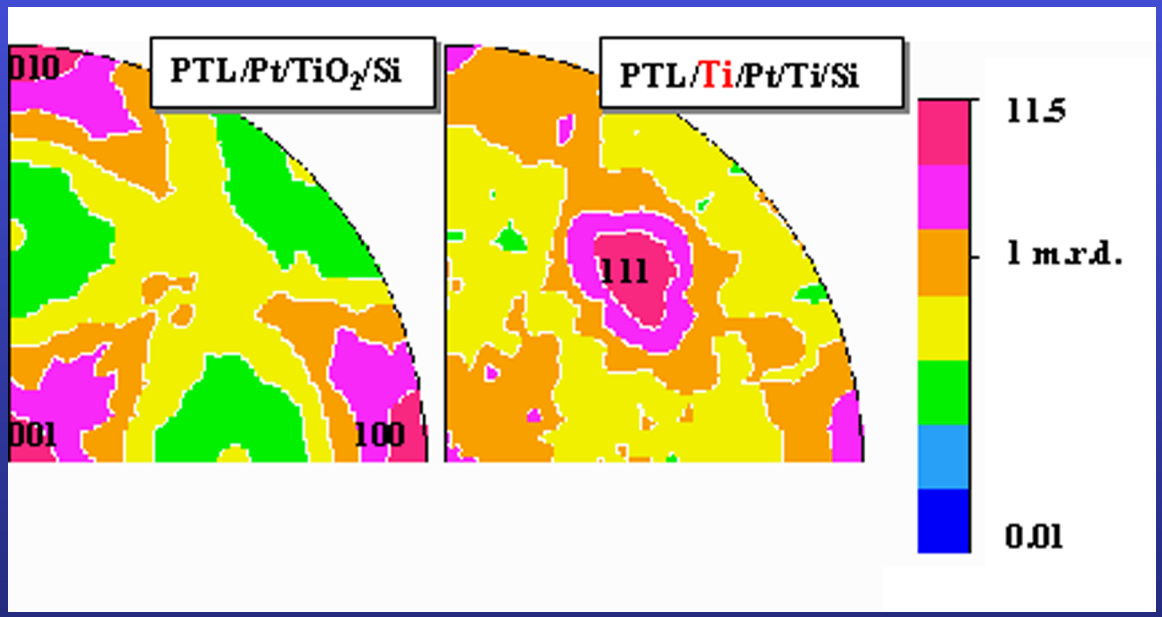

Compliance coefficients [10^{-3} GPa^{-1}]	$PbTiO_3$ single crystal (data set A)	Film random orientation	PCT-Si <001> contrib≈17%	PLT <001> contrib.≈49%	PCT-Mg <001> contrib.≈68%
s_{11}	6.5	10.1	10.5	10.0	9.7
s_{22}	6.5	10.0	10.5	10.0	9.7
s_{33}	33.3	9.8	9.0	10.3	11.3
s_{44}	14.5	13.2	12.8	12.9	13.1
s_{55}	14.5	13.2	12.8	13.0	13.1
s_{66}	9.6	13.4	14.0	13.5	12.7
s_{12}	-0.35	-3.3	-3.5	-3.2	-3.0
s_{21}	-0.35	-3.3	-3.5	-3.2	-3.0
s_{13}	-7.1	-3.2	-3.1	-3.4	-3.6
s_{31}	-7.1	-3.2	-3.1	-3.4	-3.6
s_{23}	-7.1	-3.2	-3.1	-3.4	-3.6
s_{32}	-7.1	-3.2	-3.1	-3.4	-3.6
s_{33}/s_{11}	5.1	0.97	0.86	1.03	1.16
s_{13}/s_{12}	20.3	0.97	0.89	1.06	1.20

Geometric mean average + biaxial stress state

Ferroelectric PMN-PT films

J. Ricote, DMF-Madrid

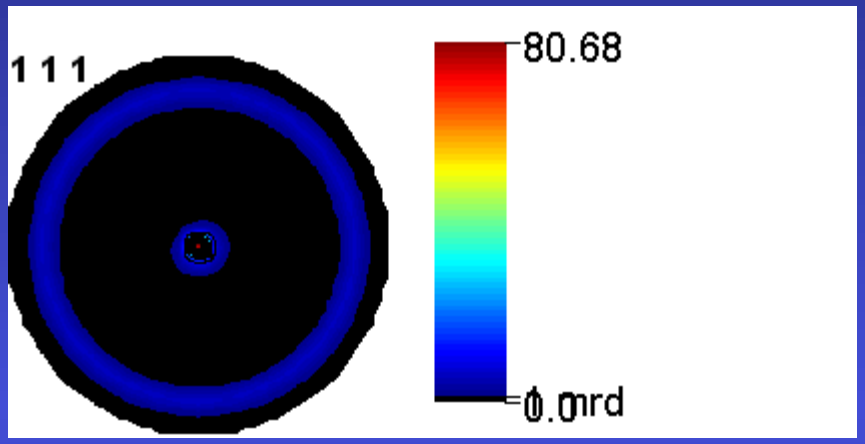

Pt

a = 3.91172(1) Å
T = 583(5) Å
t_{iso} = 960(1) Å
ε = 0.0032(1) rms
σ_{11}= 0.639(1) GPa
σ_{22}= 0.651(1) GPa
σ_{12}= -0.009(1) GPa

$Pb_{0.7}(Mg_{1/3}Nb_{2/3})O_3$-$Pb_{0.3}TiO_3$ /$Ti0_2$/Pt/Si-(100)

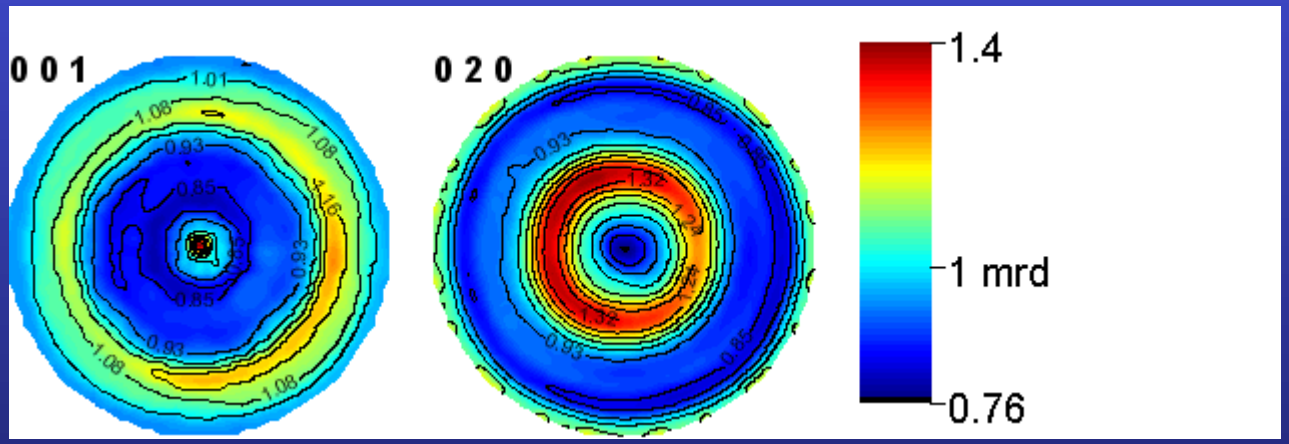

a = 5.67858(9) Å
b = 5.69038(9) Å
c = 3.99558(4) Å
β = 90.392(1) Å
T = 1322(9) Å
t_{iso} = 1338(2) Å
ε = 0.0067(1) rms

$AlN/Pt/TiO_x/Al_2O_3/Ni\text{-}Co\text{-}Cr\text{-}Al$

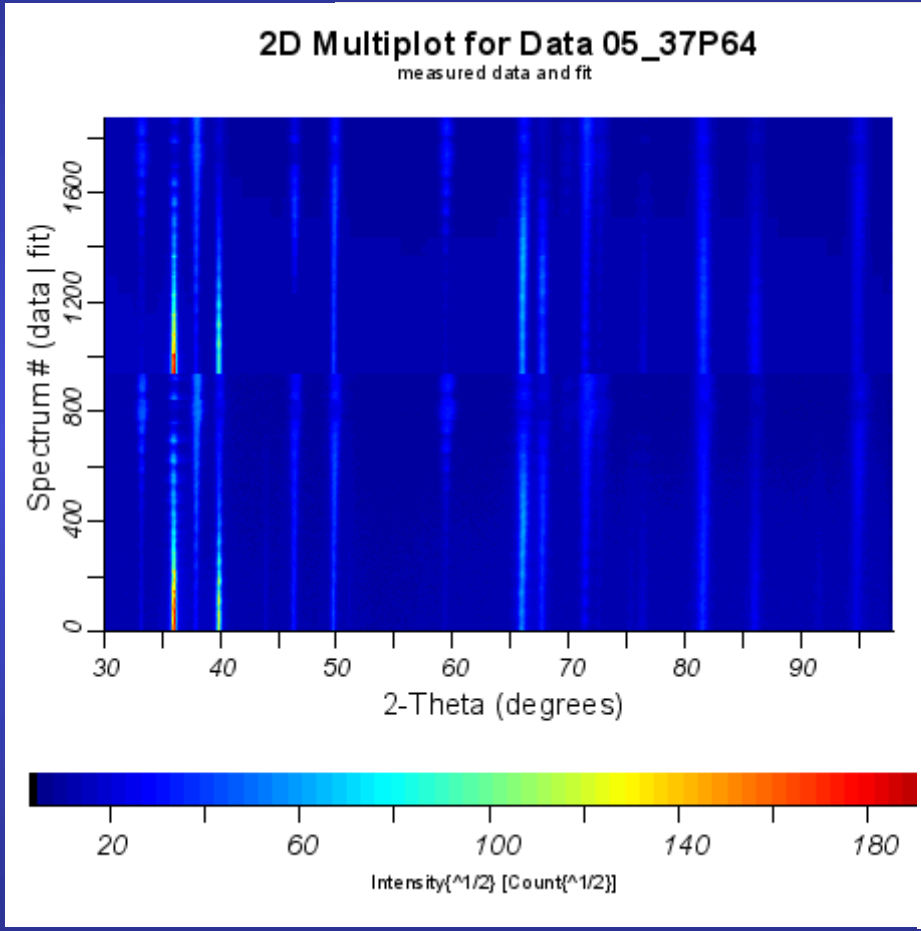

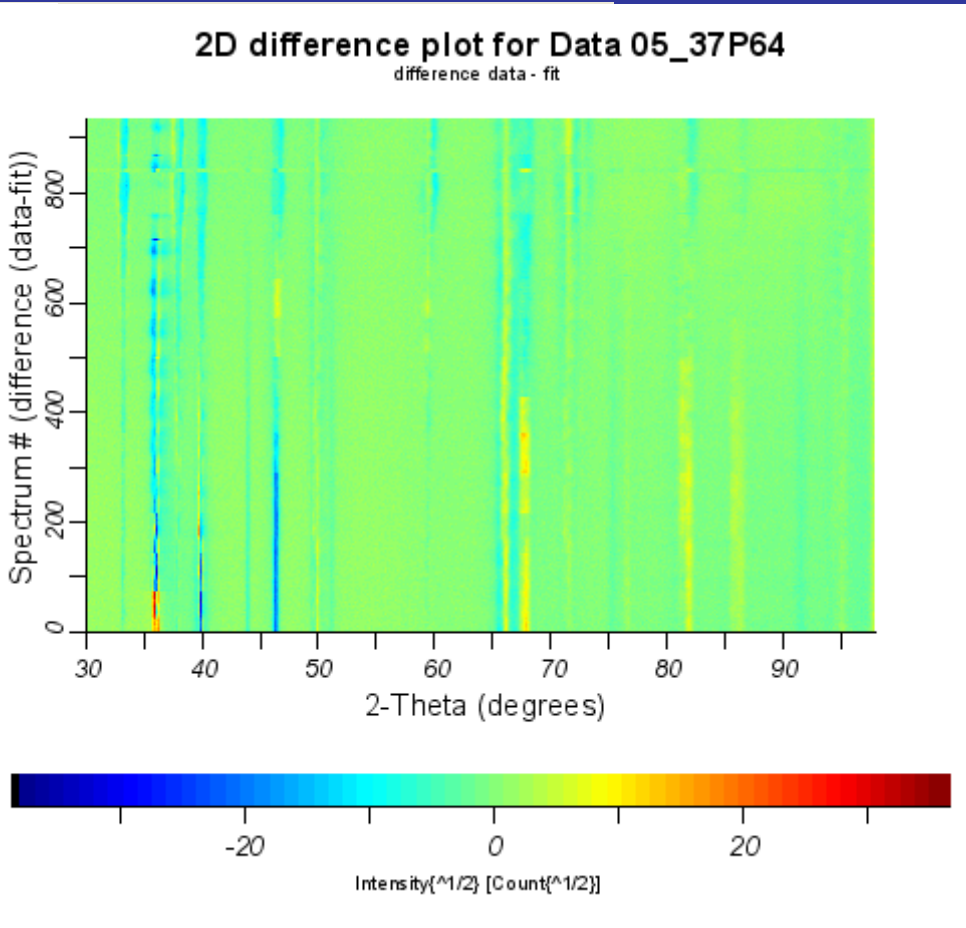

Rw (%) = 24.120445
Rexp (%) = 5.8517213

T(AlN) = 14270(3) nm
T(Pt) = 430(3) nm

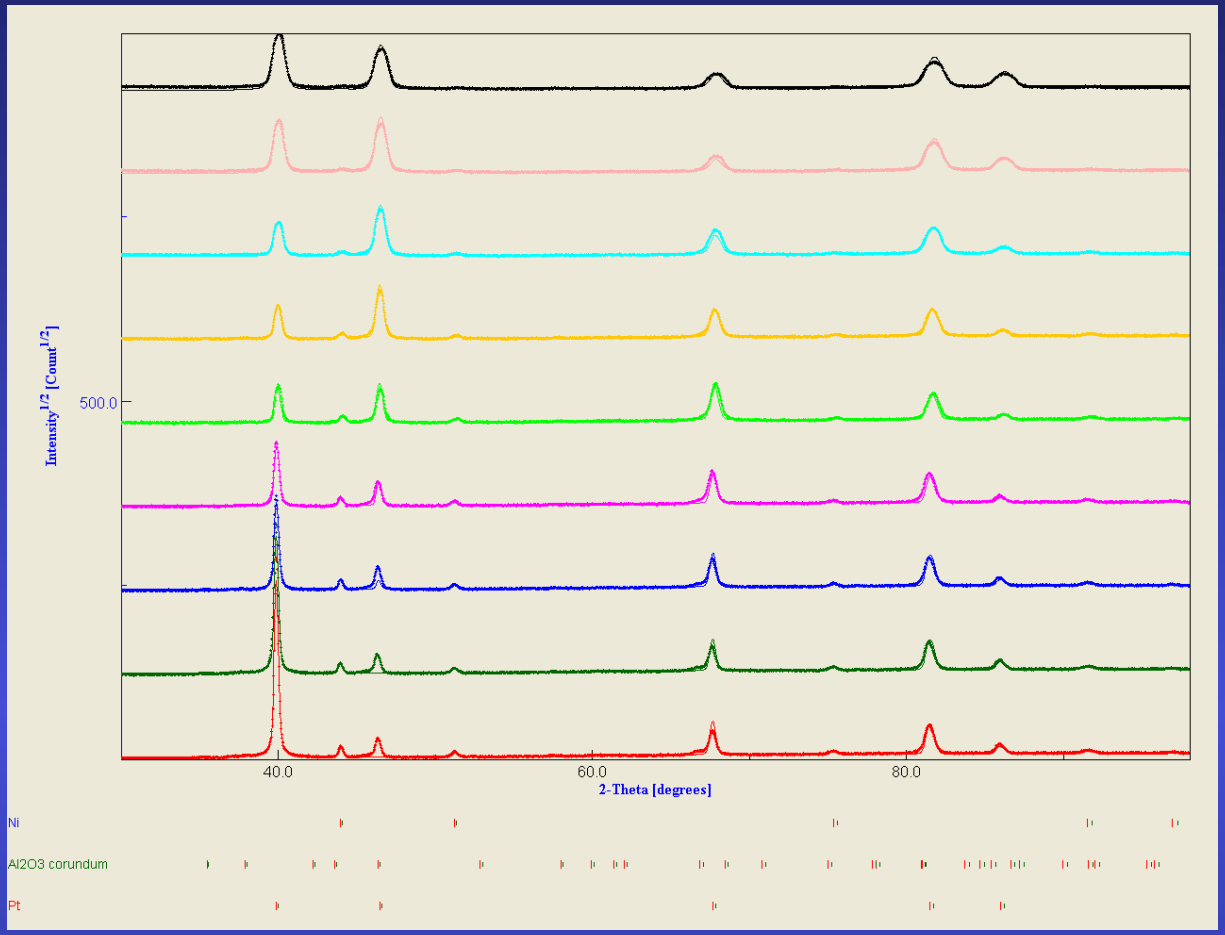

(χ,φ) randomly selected diagrams

Al_2O_3

a = 4.7562(6) Å
c = 12.875(3) Å
T= 7790(31) nm
<t> = 150(2) Å
<ε> = 0.008(3)

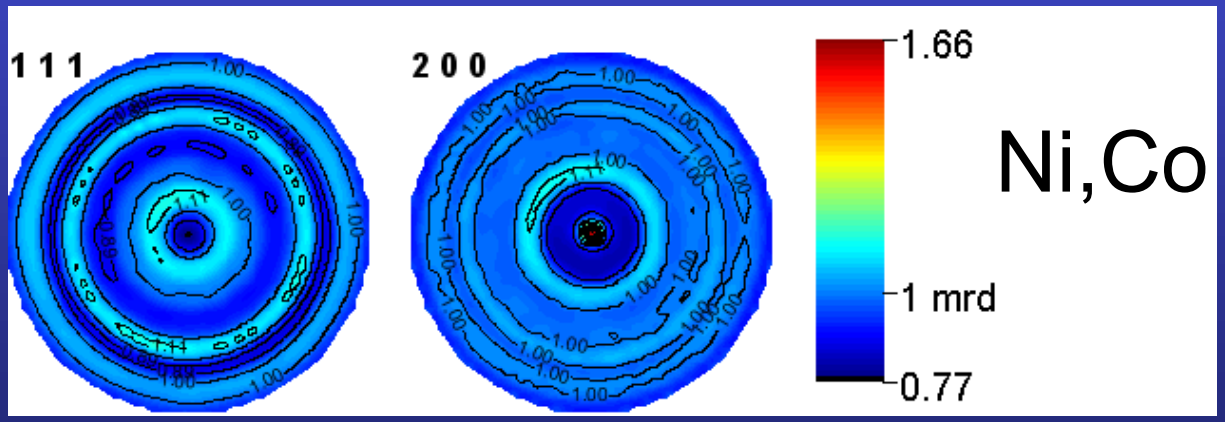

a = 3.569377(5) Å
<t> = 7600(1900) Å
<ε> = 0.00236(3)
σ_{11} = -328(8) MPa
σ_{22} = -411(9) MPa

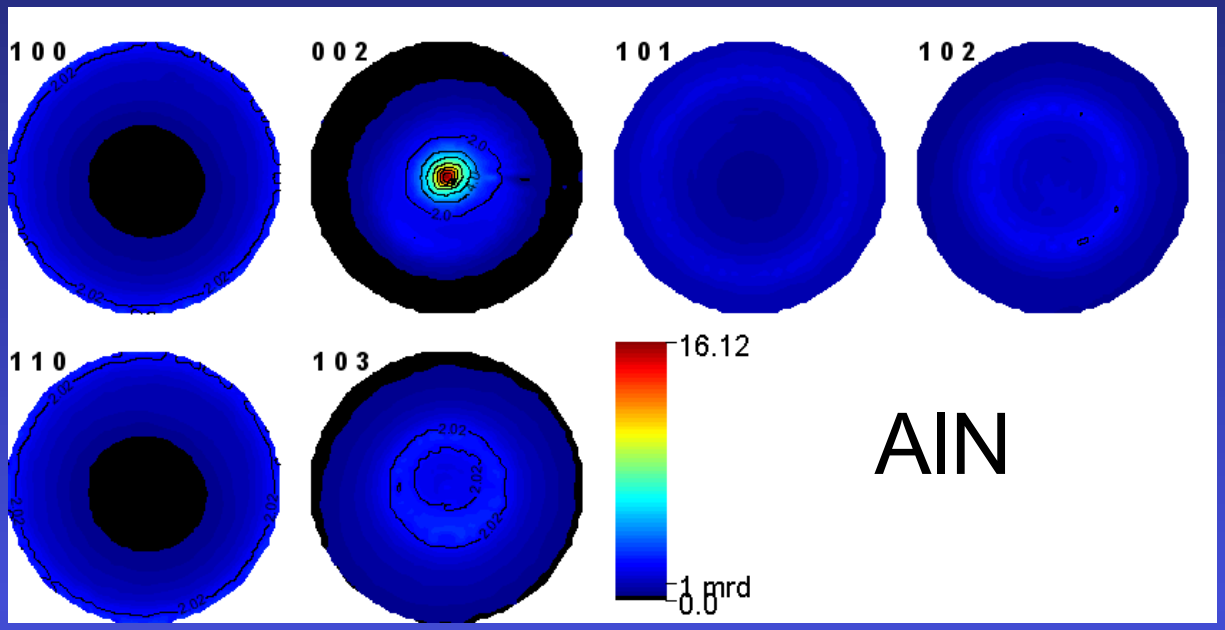

Rw (%) = 4.1

a = 3.11203(1) Å
c = 4.98252(1) Å
T = 14270(3) nm
<t> = 2404(8) Å
<ε> = 0.001853(2)
σ_{11} = -1019(2) MPa
σ_{22} = -845(2) MPa

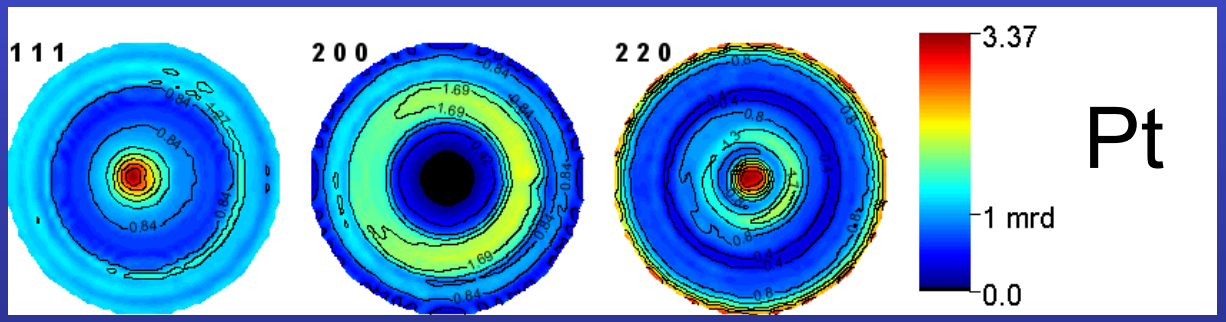

Rw (%) = 33.3

a = 3.91198(1) Å
T = 1204(3) nm
<t> = 2173(10) Å
<ε> = 0.002410(3)
σ_{11} = -196.5(8)
σ_{22} = -99.6(6)

Substrate bias vs stress-texture evolution

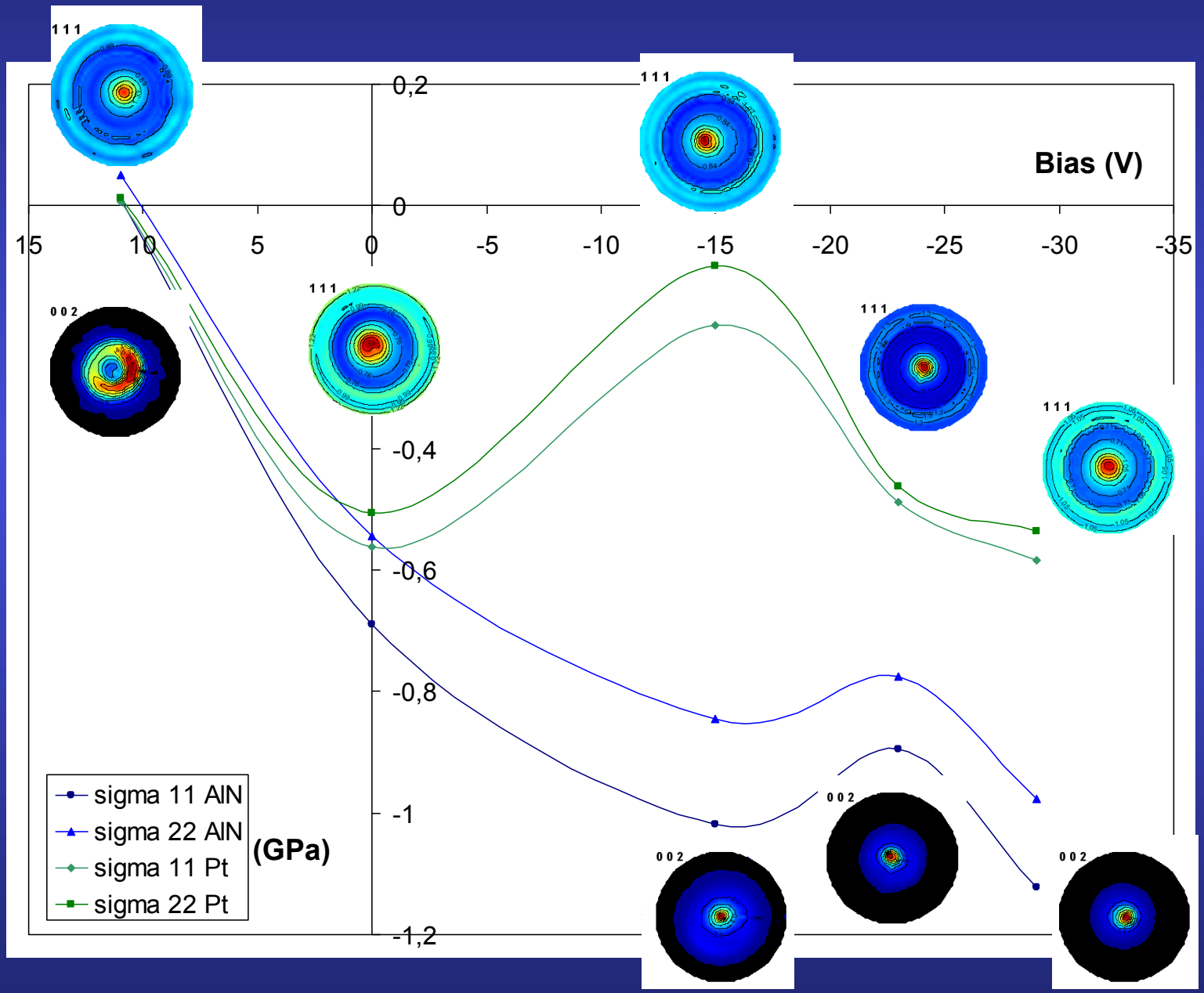

Si nanocrystalline thin films

M. Morales, Caen

Silicon thin films deposition by reactive magnetron sputtering:

- power density 2W/cm^2
- total pressure: $p_{total} = 10^{-1}$ Torr
- plasma mixture: H_2 / Ar, $pH_2 / p_{total} = 80$ %
- temperature: 200°C
- substrates: amorphous SiO_2 (a-SiO_2)
  (100)-Si single-crystals
- target-substrate distance (d)
  - a-SiO_2 substrates: d = 4, 6, 7, 8, 10, 12 cm
    films A, B, C, D, E, F
  - (100)-Si: d = 6, 12 cm
    films G, H

Aim: quantum confinement, photoluminescence properties

Typical refinement

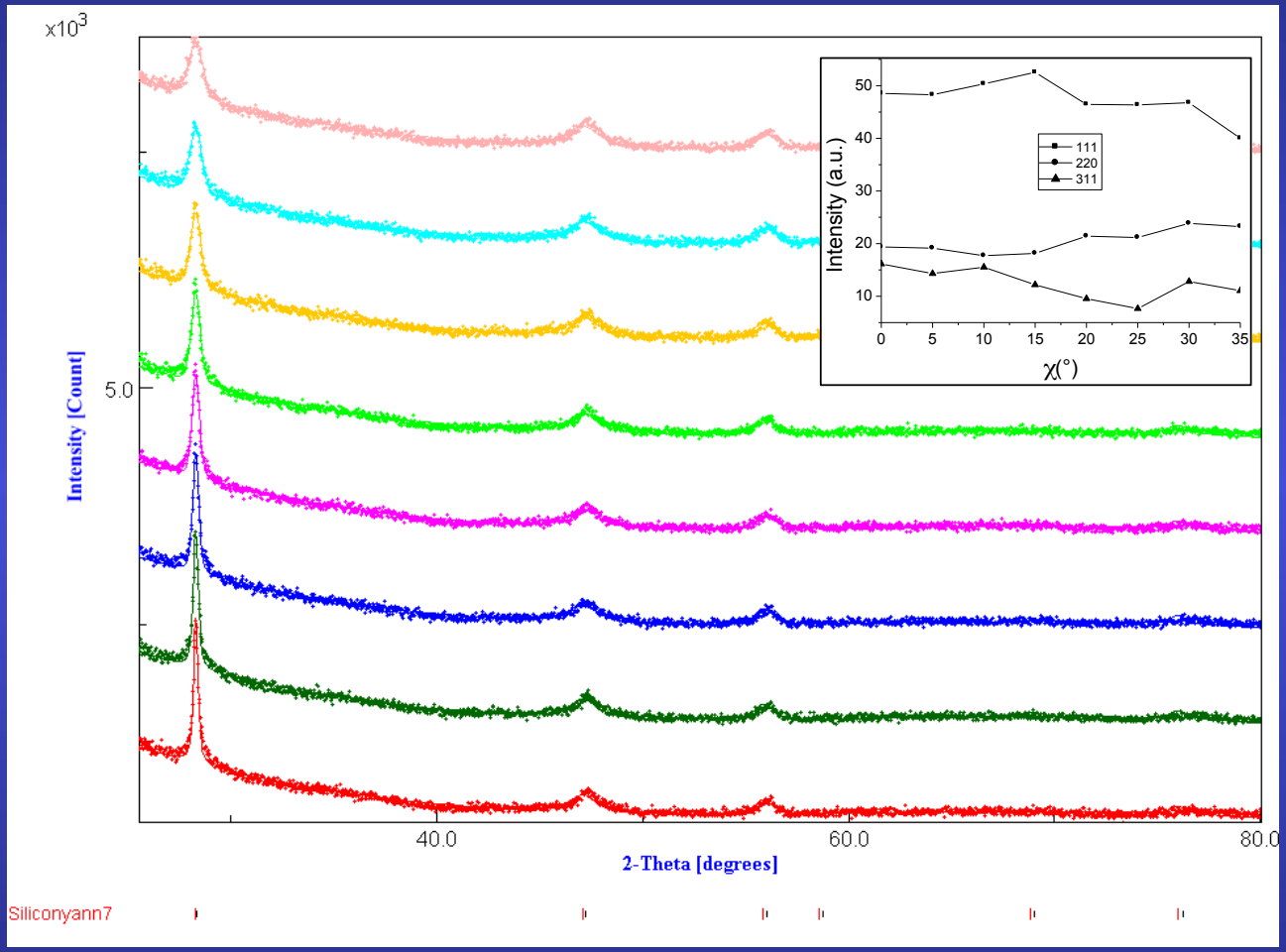

broad, anisotropic diffracted lines, textured samples

Refinement Results

Sample	d (cm)	a (Å)	RX thickness (nm)	Anisotropic sizes (Å)			Texture parameters			Reliability factors (%)			
				<111>	<220>	<311>	Maximum (m.r.d.)	minimum (m.r.d.)	Texture index F^2 (m.r.d^2)	RP_0	R_w	R_B	R_{exp}
A	4	5.4466 (3)	---	94	20	27	1.95	0.4	1.12	1.72	4.0	3.7	3.5
B	6	5.4439 (2)	711 (50)	101	20	22	1.39	0.79	1.01	0.71	4.9	4.3	4.2
C	7	5.4346 (4)	519 (60)	99	40	52	1.72	0.66	1.05	0.78	4.3	4.0	3.9
D	8	5.4461 (2)	1447 (66)	100	22	33	1.57	0.63	1.04	0.90	5.5	4.6	4.5
E	10	5.4462 (2)	1360 (80)	98	20	25	1.22	0.82	1.01	0.56	5.0	3.9	4.0
F	12	5.4452 (3)	1110 (57)	85	22	26	1.59	0.45	1.05	1.08	4.2	3.5	3.7
G	6	5.4387 (3)	1307 (50)	89	22	28	1.84	0.71	1.01	1.57	5.2	4.7	4.2
H	12	5.4434 (2)	1214 (18)	88	22	24	2.77	0.50	1.12	2.97	5.0	4.5	4.3

Mean anisotropic shape

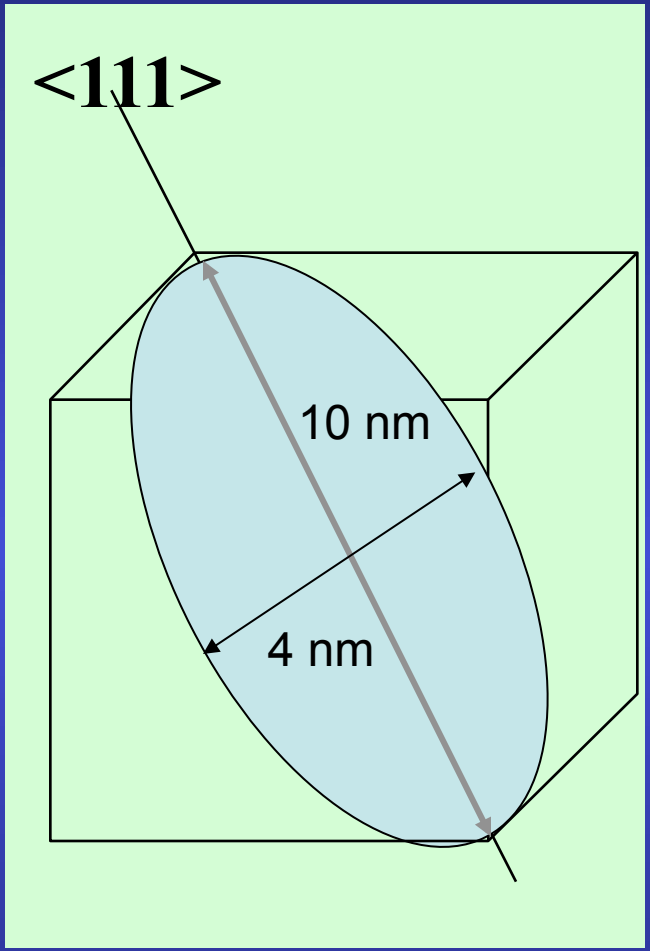

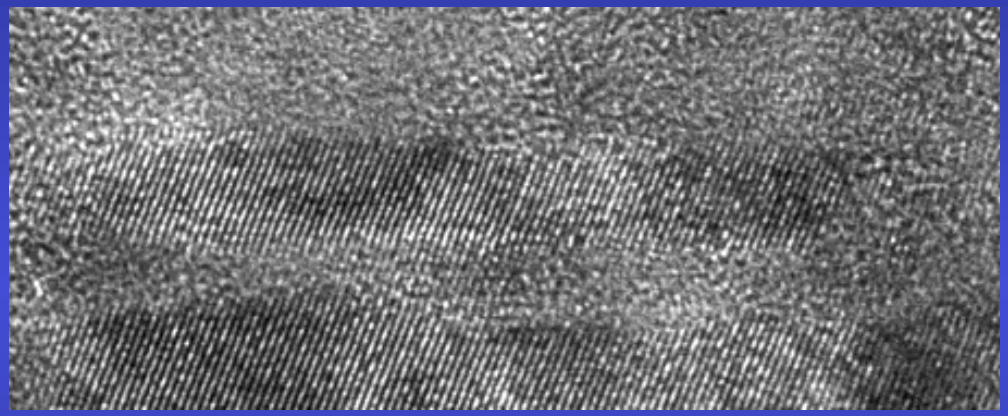

Schematic of the mean crystallite shape for Sample D represented in a cubic cell, as refined using the Popa approach and exhibiting a strong elongation along <111>, and TEM image

001 Inverse Pole Figures

a-SiO_2

(100)-Si

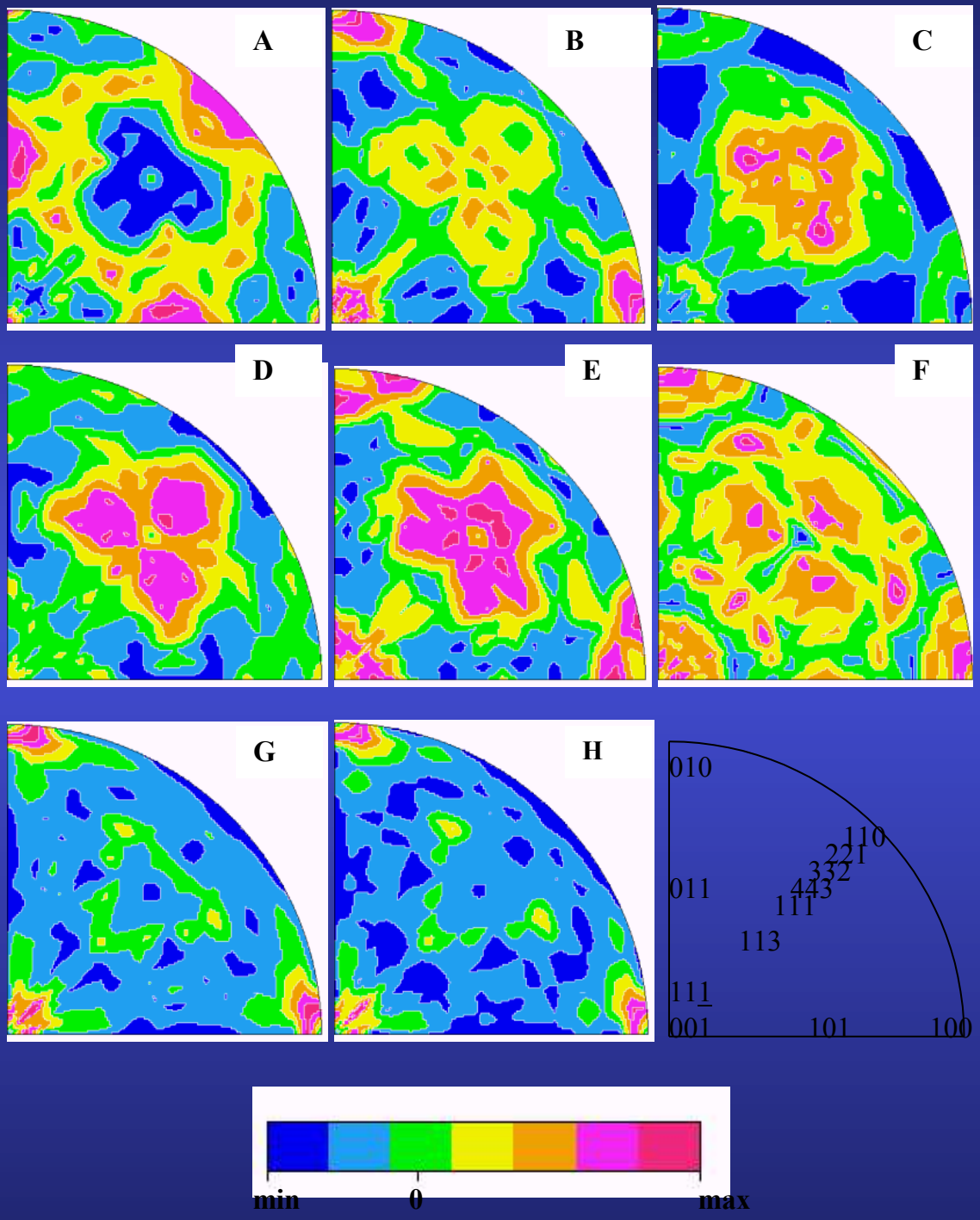

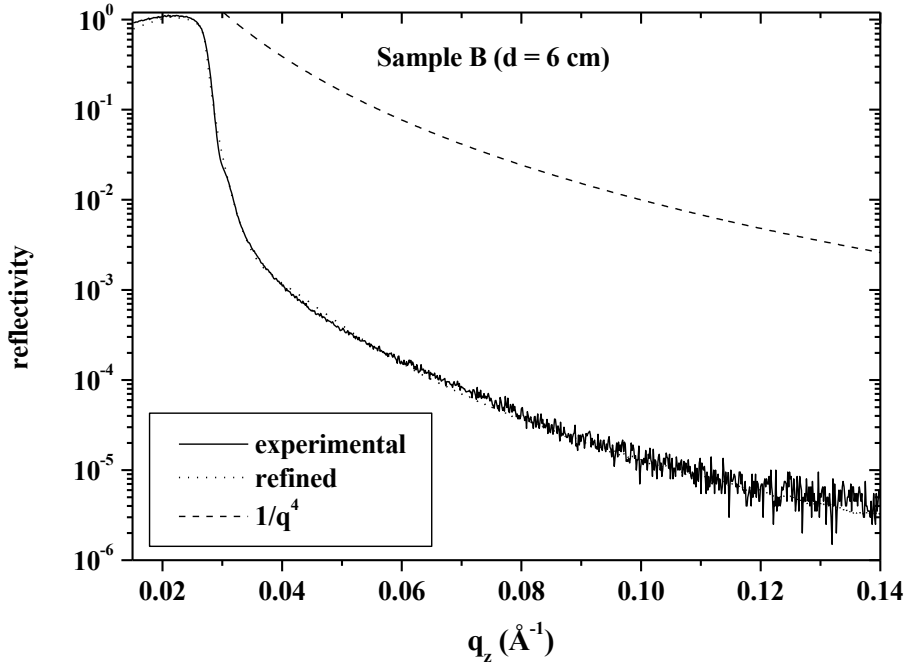

XRR:

Roughness governed

AFM:

homogeneous roughness

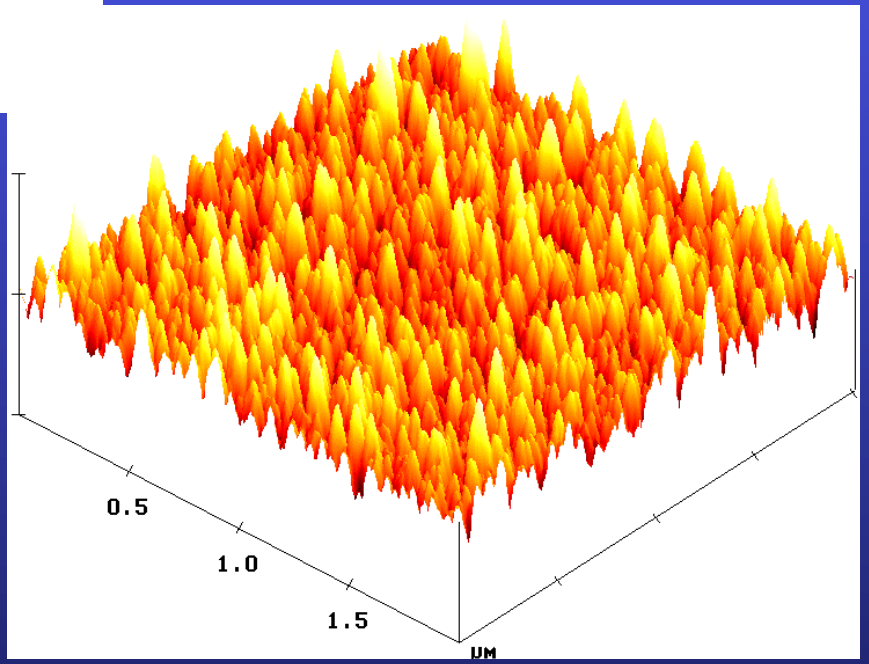

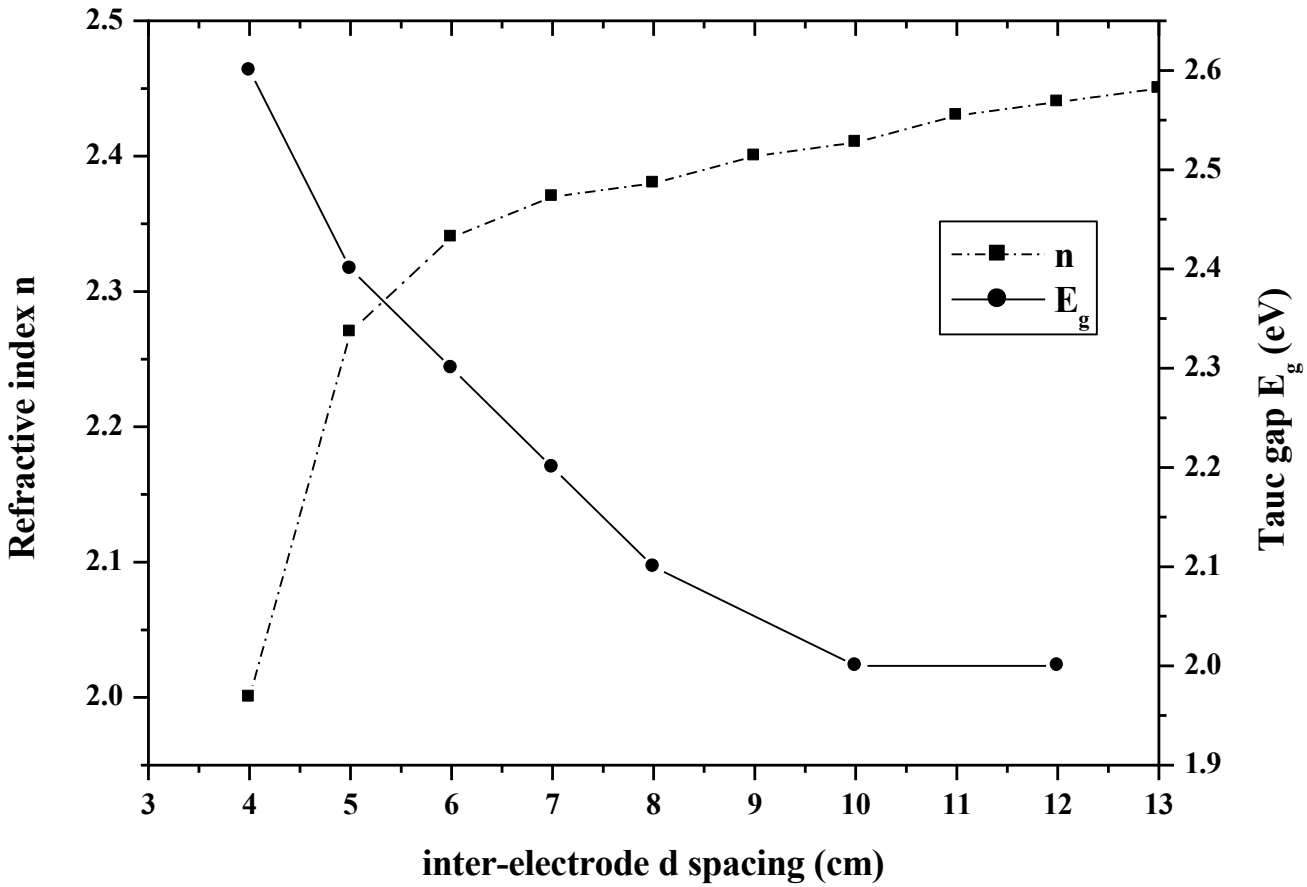

↳ Refractive index linked to film porosities:

Larger target-sample distances: increased compacity due to lower nanopowder filling

ZnSe:Cr^{2+} films
M. Morales, CIMAP

conditions:

- $20 \leq T_d \leq 385°C$
- P_{RF} = 50-200W
- P_{Ar} = 0.5 Pa and 2 Pa
- d = 7 and 10 cm

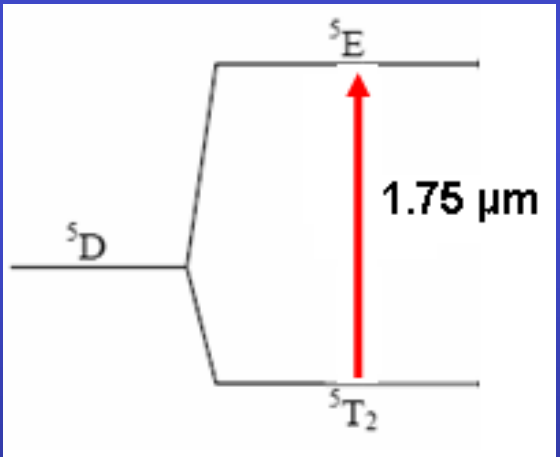

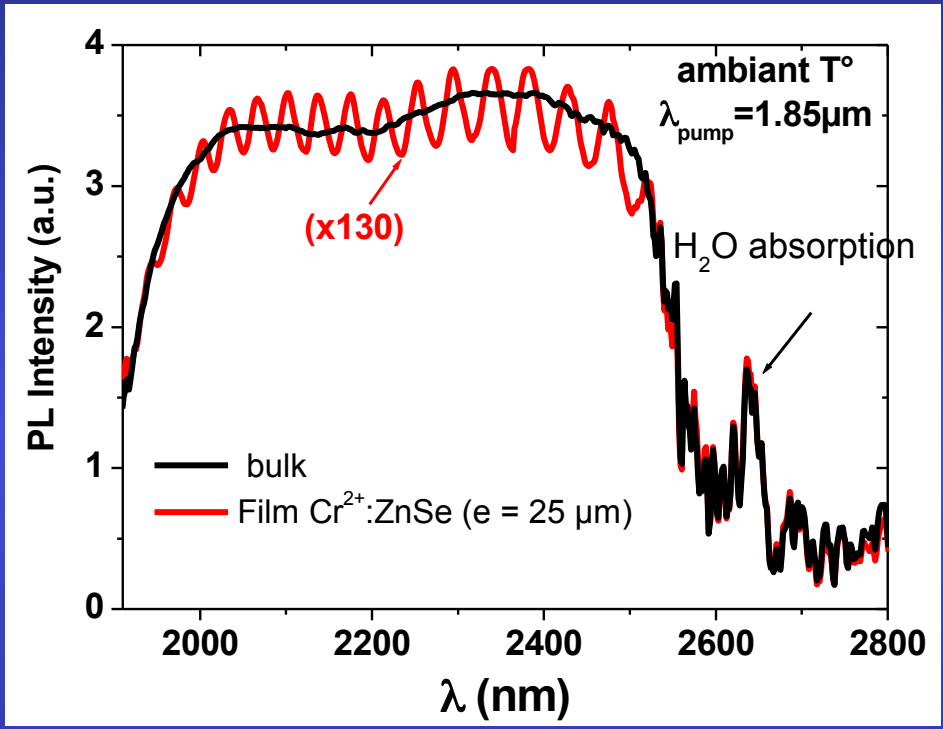

- Large emission band centred at 2200nm: $^5E \rightarrow {}^5T_2$ transition (Cr^{2+})
- Single crystals and thin films: similar spectra

111 Peak shifts

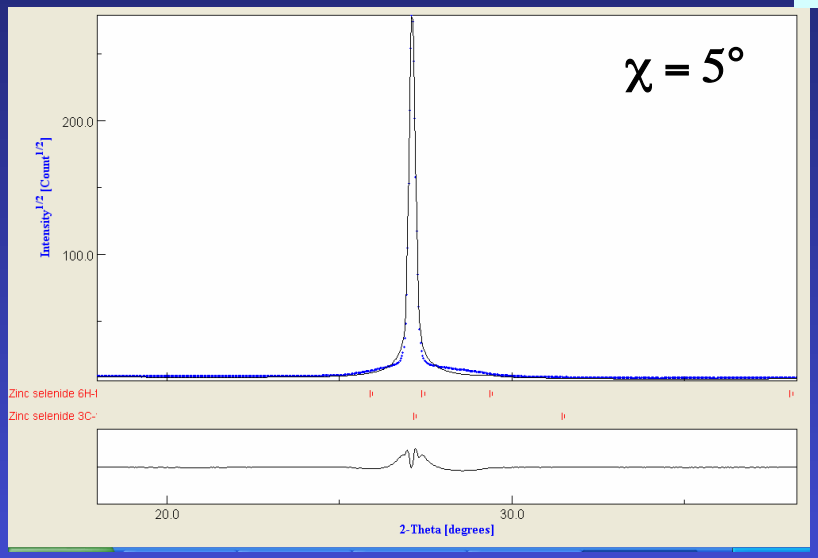

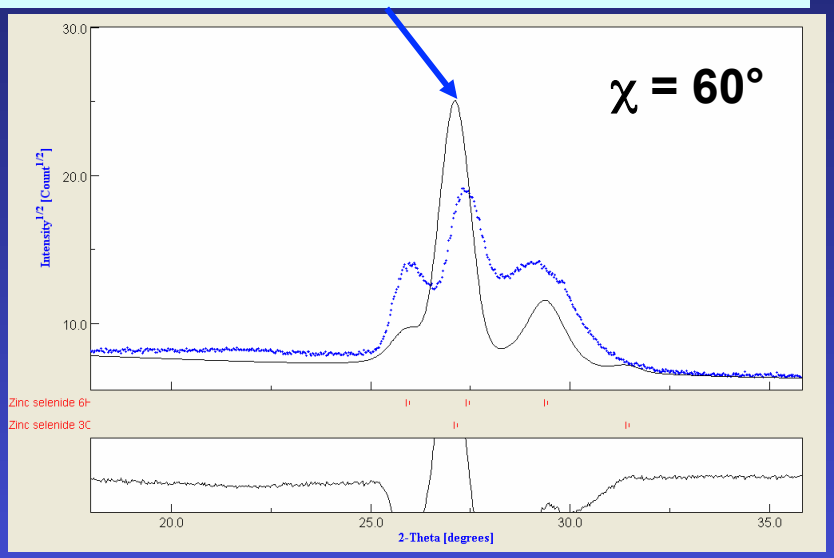

Residual stresses and/or stacking faults

Anisotropic sizes

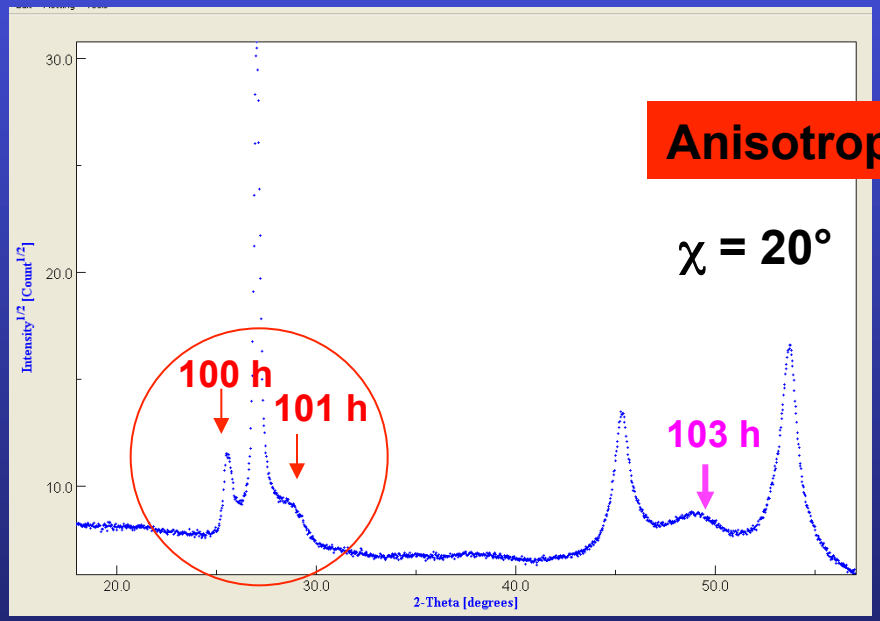

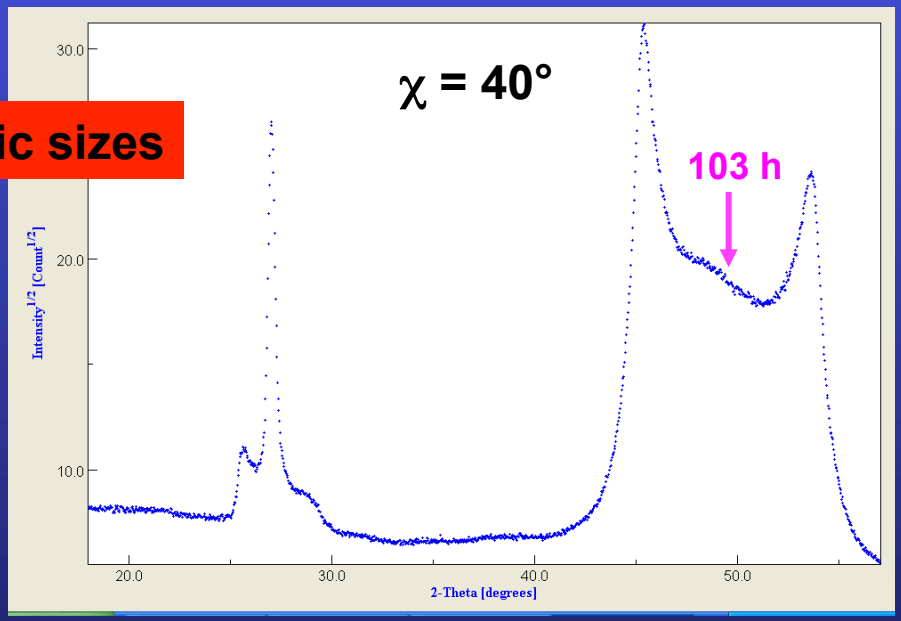

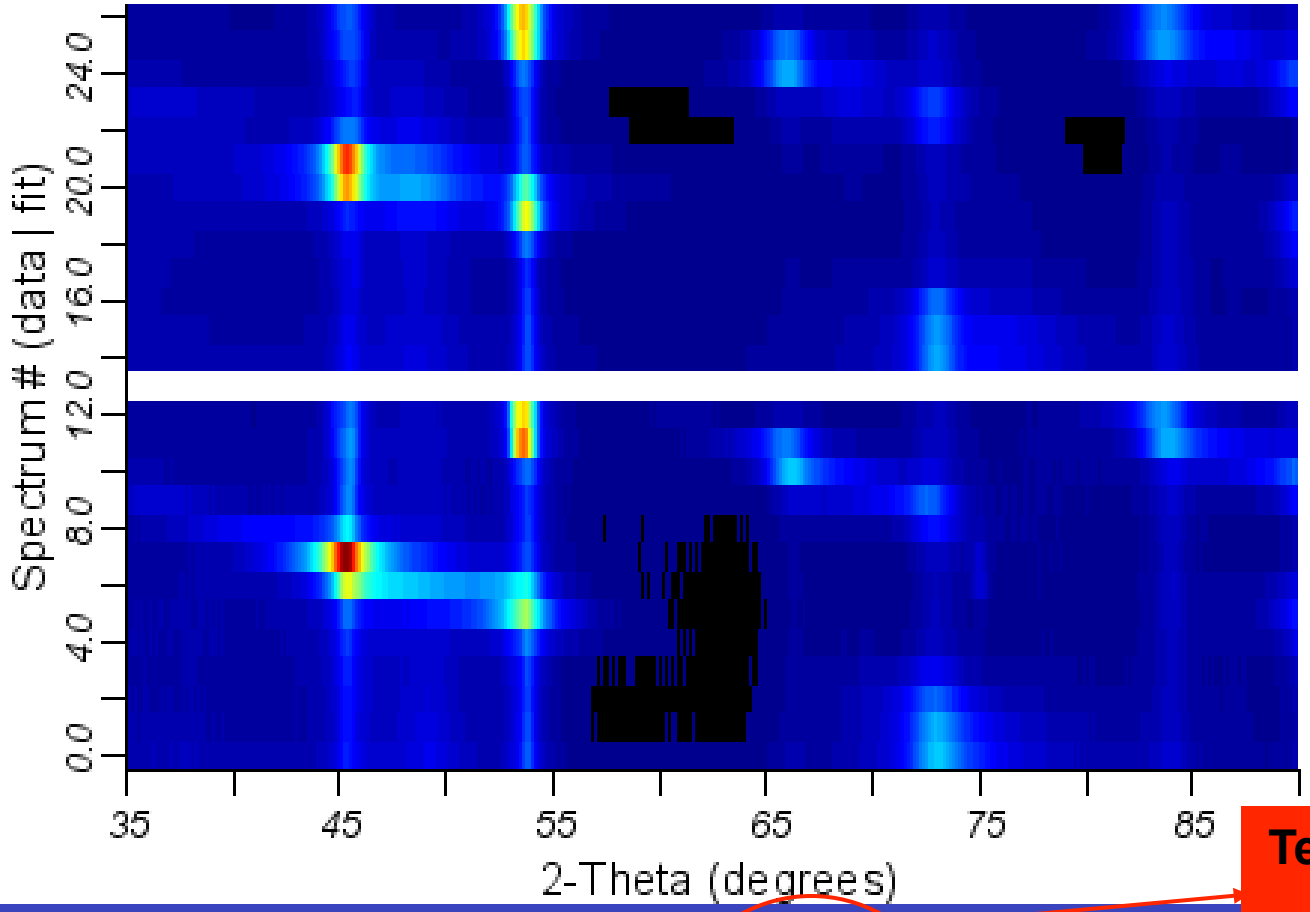

R_{exp} = 11.1%
R_W = 25.7%

% H-ZnSe = 45.4%

Tensile in plane stress ≠ Rizzo et al.

Phase	Cell parameters (Å)	In-plane stress (MPa)	Anisotropic sizes (Å)			
			[111]	[100]	[110]	[103]
C-ZnSe	a = 5.6497(3)	263 (14)	112 (1)	117 (5)	85(1)	-
H-ZnSe	a= 3.9527(6) c = 6.7154(8)	436 (25)	-	244 (1)	244 (2)	20(2)

C-ZnSe texture :

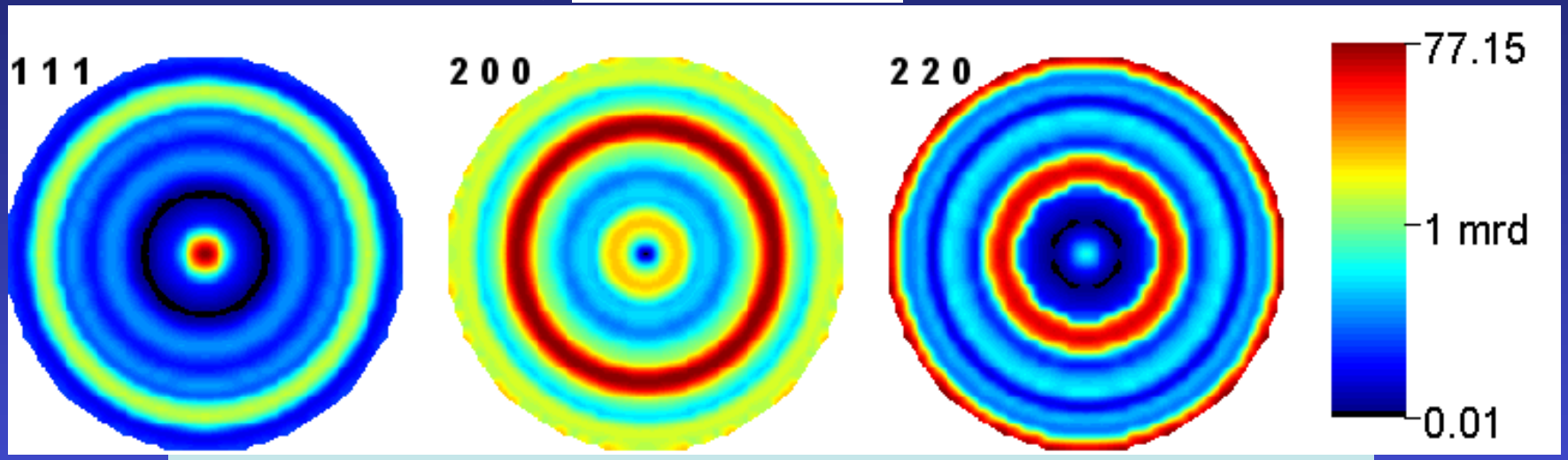

strong <111> fibre texture with some residual orientations

H-ZnSe texture :

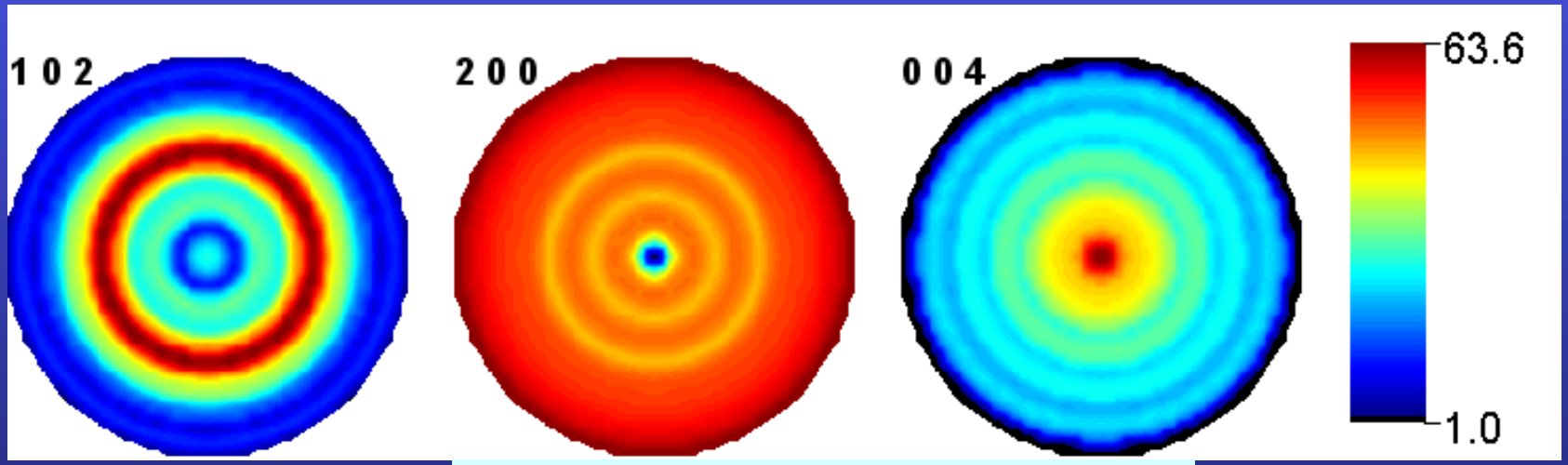

unique <001> strong fibre texture

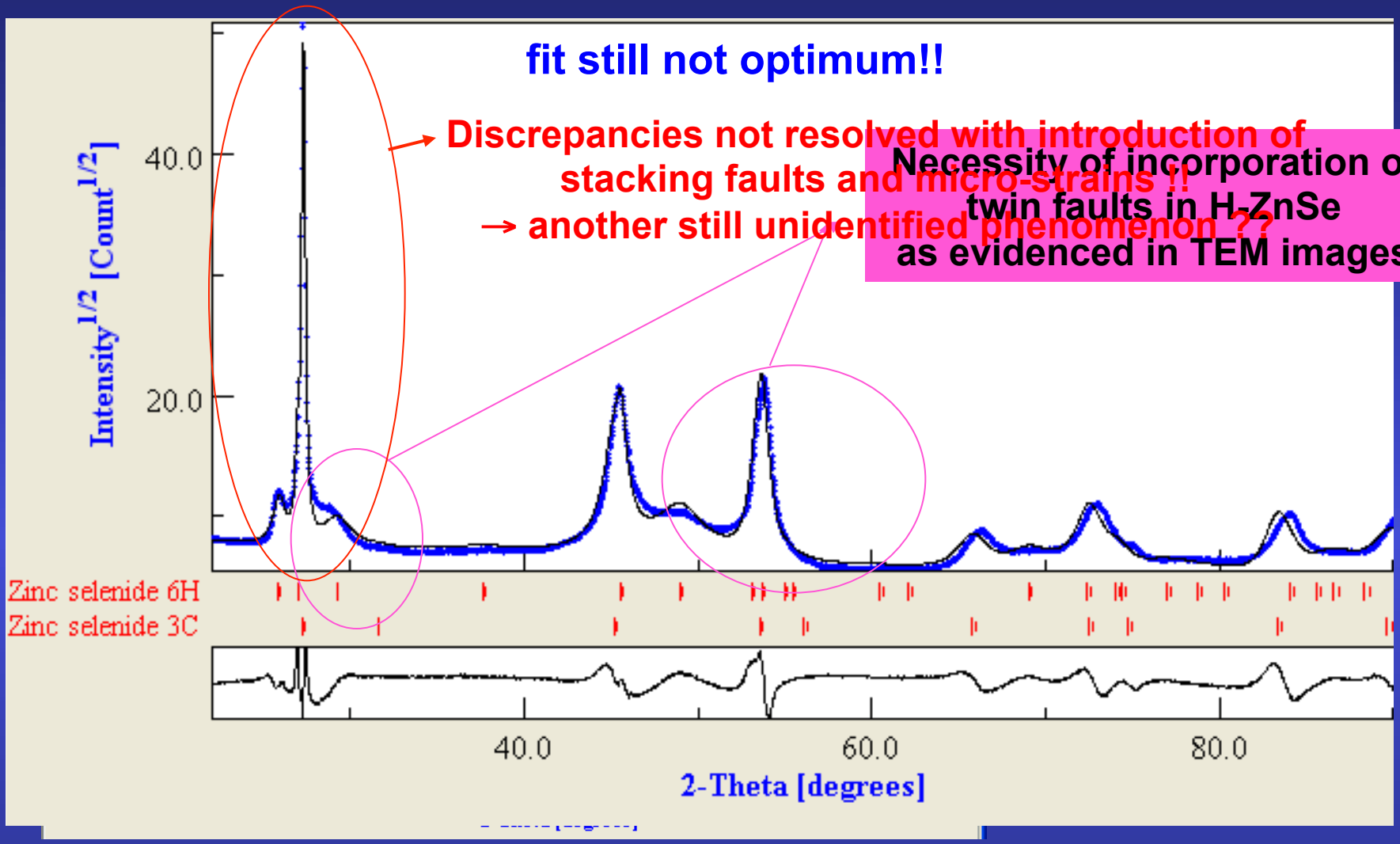

Better reproduction for 2θ > 35° with H-ZnSe twin faults probability of 45.7 (6)%;
but still discrepancies for 2θ < 35°

Turbostratic phyllosilicate aggregates

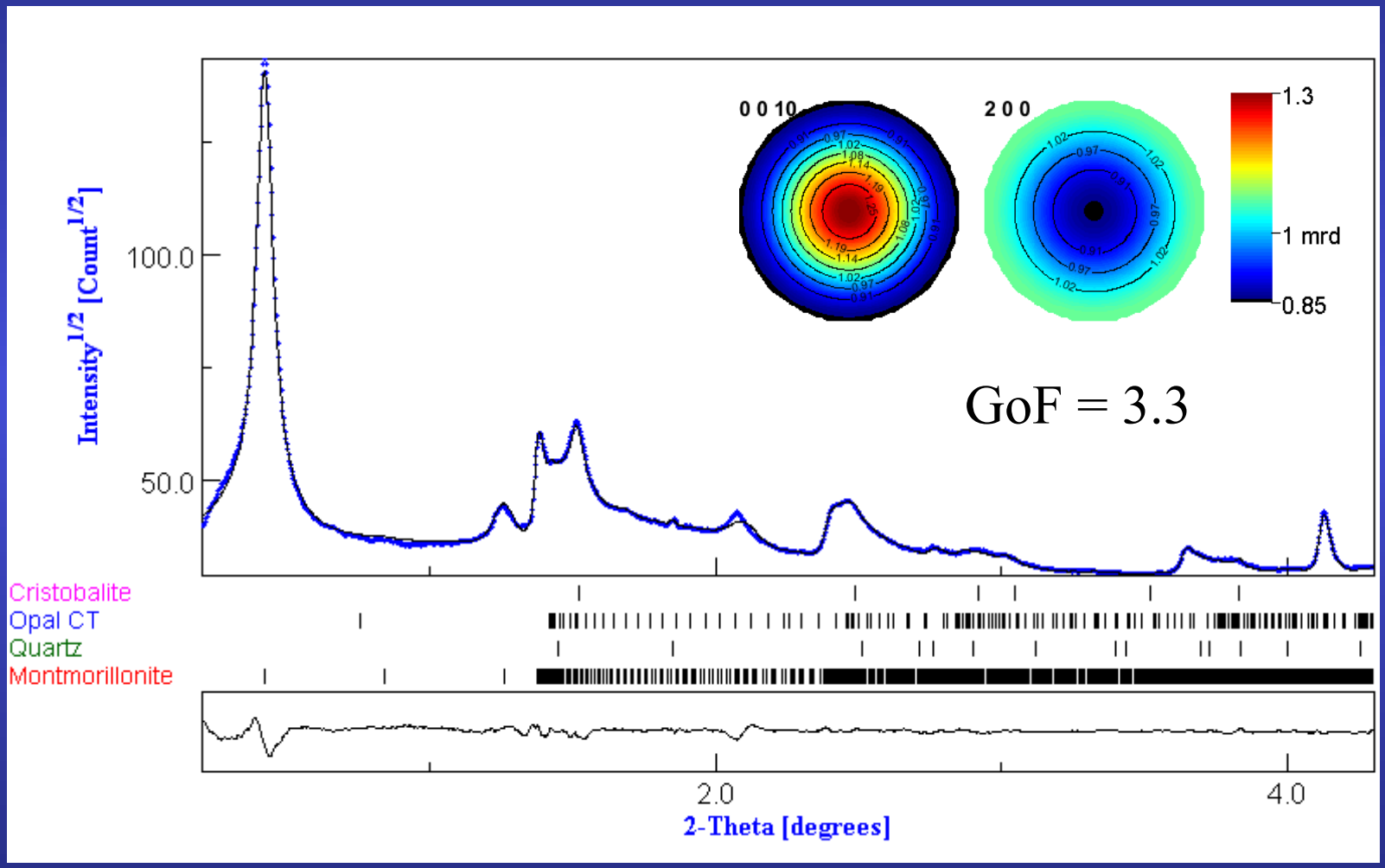

V%
1.45(2)
6.6(1)
0.19(1)
91.8(3)

Independent measurements

Different wavelengths and rays

Reflectivity: thickness, roughness, electron density profiles

X-ray Fluorescence: composition

Spectroscopies: local structures (PDF, FTIR, Mossbauer …), eventually anisotropic (P-EXAFS, ESR, Raman …), Element profiles (SIMS, RBS …) …

Physical models: magnetisation, conductivity …

Environments: applied fields

Specular reflectivity: **q**=(0,0,z)

- Fresnel:

$$R(\mathbf{q}) = \left| \frac{q_z - \sqrt{q_z^2 - q_c^2 + \frac{32i\pi^2\beta}{\lambda^2}}}{q_z + \sqrt{q_z^2 - q_c^2 + \frac{32i\pi^2\beta}{\lambda^2}}} \right|^2 \delta q_x \delta q$$

- matrix:

$$R^{flat} = \frac{r_{0,1}^2 + r_{1,2}^2 + 2r_{0,1}r_{1,2}\cos 2k_{Z,1}h}{1 + r_{0,1}^2 r_{1,2}^2 + 2r_{0,1}r_{1,2}\cos 2k_{Z,1}h}$$

- Born approximation:
  Electron Density Profile

$$R(q_z) = r.r^* = R_F(q_z)\left| \frac{1}{\rho_s} \int_{-\infty}^{+\infty} \frac{d\rho(z)}{dz} e^{iq_z z} dz \right|^2$$

- Roughness:

$$R^{rough}(q_z) = R(q_z)\exp(-q_{z,0}q_{z,1}\sigma^2) \quad \text{Low-angles (reflectivity)}$$

$$S_R = 1 - p\exp(-q) + \mathrm{p}\exp\left(\frac{-\mathrm{q}}{\sin\theta}\right) \quad \text{high-angle (Suortti)}$$

CPS scans

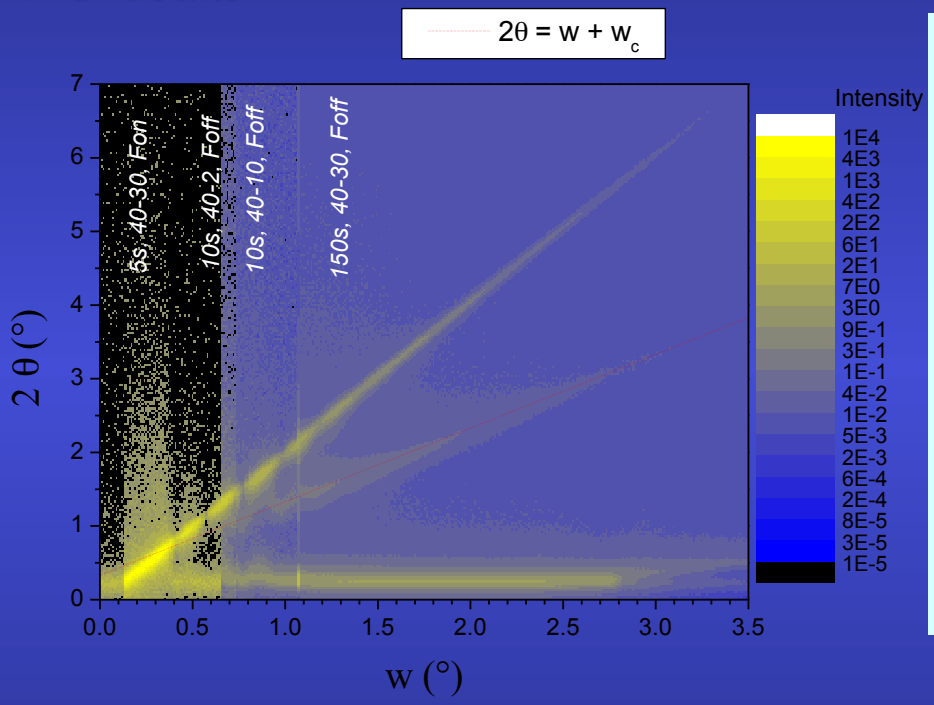

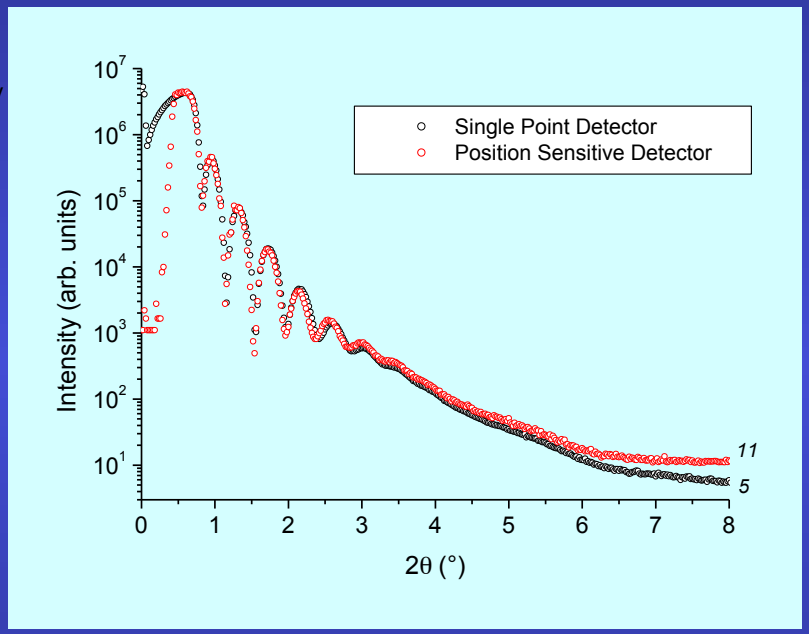

Useful for having bot specular and off-specular signals in one scan

Microstructure of nanocrystalline materials: TiO_2 rutile [1]

- *quantitative analysis of electron diffraction ring pattern ?*

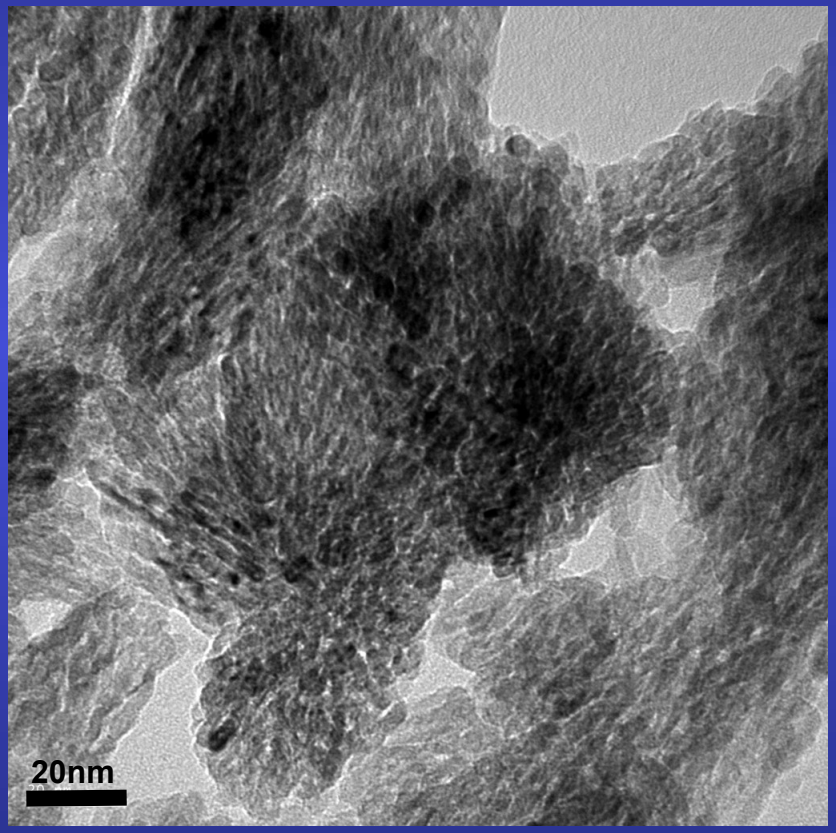

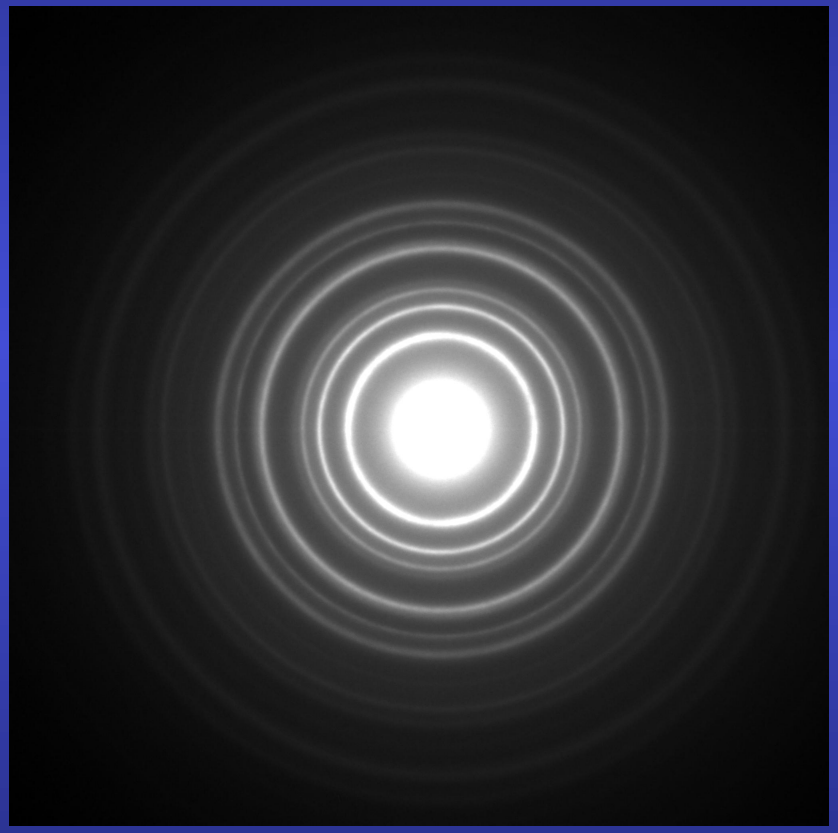

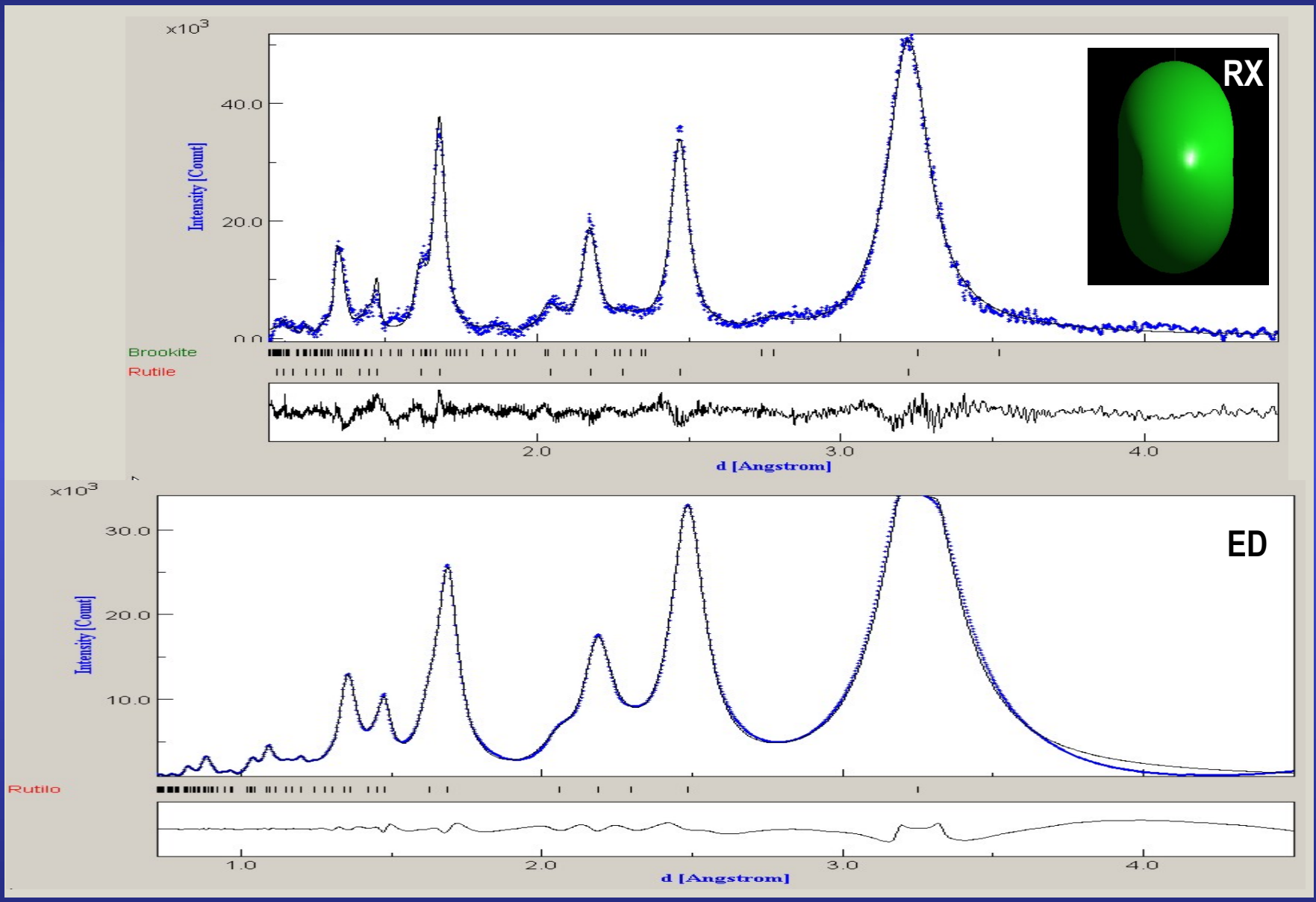
x10^3
40.0
20.0
0.0
Intensity [Count]
RX
Brookite
Rutile
2.0
3.0
4.0
d [Angstrom]
x10^3
30.0
20.0
10.0
Intensity [Count]
ED
Rutilo
1.0
2.0
3.0
4.0
d [Angstrom]

Why not more ?

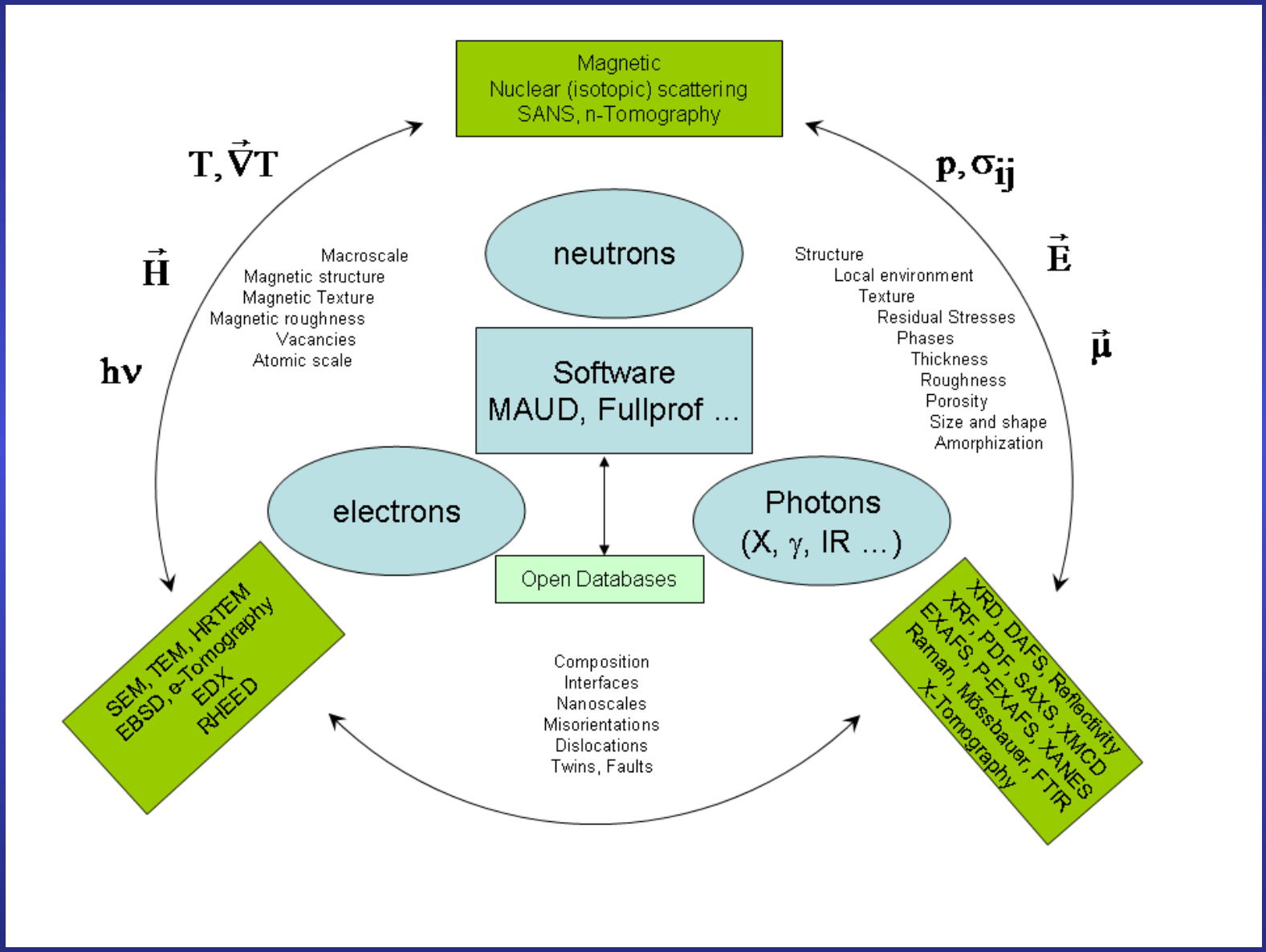
Magnetic
Nuclear (isotopic) scattering
SANS, n-Tomography
$T, \vec{\nabla}T$
p, σ_{ij}
$\vec{H}$
$\vec{E}$
$h\nu$
$\vec{\mu}$
Macroscale
Magnetic structure
Magnetic Texture
Magnetic roughness
Vacancies
Atomic scale
neutrons
Structure
Local environment
Texture
Residual Stresses
Phases
Thickness
Roughness
Porosity
Size and shape
Amorphization
Software
MAUD, Fullprof ...
electrons
Photons
(X, γ, IR ...)
Open Databases
SEM, TEM, HRTEM
EBSD, e-Tomography
EDX
RHEED
XRD, DAFS, Reflectivity
XRF, PDF, SAXS, XMCD
EXAFS, P-EXAFS, XANES
Raman, Mössbauer, FTIR
X-Tomography
Composition
Interfaces
Nanoscales
Misorientations
Dislocations
Twins, Faults

Conclusions

a) A lot of dilemma are only apparent

b) Texture helps to resolve them: good for real samples

c) Anisotropy favours higher resolutions

d) Combined analysis may be a solution, unless you can destroy your sample or are not interested in macroscopic anisotropy ...

e) If you think you can destroy it, perhaps think twice

f) more information is always needed: why not more?

g) Combined Analysis (D. Chateigner Ed), Wiley-ISTE 2010